AD-A116 966 PENNSYLVANIA UNIV PHILADELPHIA DEPT OF MATERIALS SCI--ETC F/G 11/6
EFFECTS OF RESIDUAL IMPURITIES ON HYDROGEN ASSISTED CRACKING IN--ETC(U)
JUN 82 N BANDYOPADHYAY, C J MCMAHON N00019-79-C-0523

UNCLASSIFIED NL

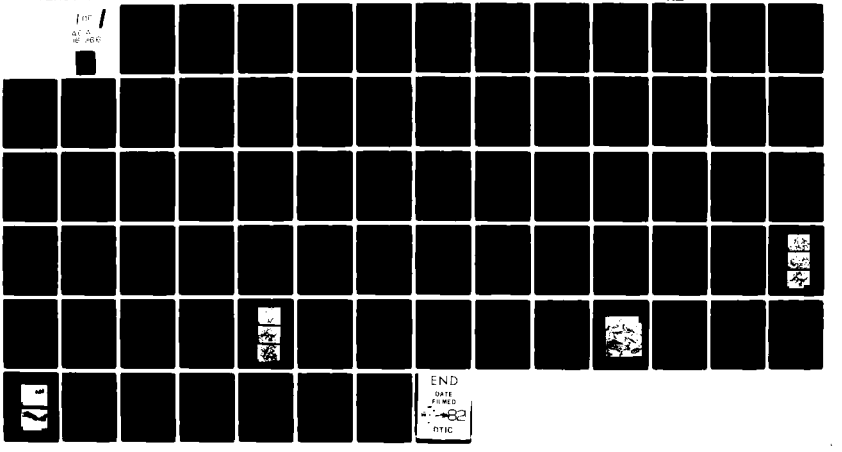

END
DATE FILMED
-82
DTIC

NAVAL AIR SYSTEMS COMMAND

OFFICE OF NAVAL RESEARCH

CONTRACT N00019-79-C-0523

TECHNICAL REPORT

PART II

EFFECTS OF RESIDUAL IMPURITIES ON HYDROGEN ASSISTED CRACKING IN HIGH STRENGTH STEELS

BY

N. BANDYOPADHYAY

AND

C. J. MCMAHON, JR.

DEPARTMENT OF MATERIALS SCIENCE AND ENGINEERING

SCHOOL OF ENGINEERING AND APPLIED SCIENCE

UNIVERSITY OF PENNSYLVANIA

PHILADELPHIA, PENNSYLVANIA

JUNE 1982

Introduction

It is now well known that hydrogen when absorbed in mild steels, quenched and tempered steels, stainless steels and nickel base (Fe-Ni-Cr) alloys, can result in a loss in ultimate tensile strength, tensile ductility, such as elongation at fracture and percent reduction in area at fracture, and in the occurrence of subcritical crack growth.

Hydrogen can be introduced into the metals and alloys in a number of ways and is often a source of problems in industries such as:

a) Nuclear Power Industry, where most of the failures in one or more components of the reactor occur in systems exposed to either light or heavy water (D_2O) in the form of liquid or steam.

b) Chemical Industry, where the components are often victimised by crevice and pitting corrosion of a plate heat exchanger, gas cooler tube sheet, caustic solution and other gas storage tanks and pipe lines, welded tubes, etc. Plating of steel with chromium, cadmium, etc. can also result in hydrogen production and absorption in steels.

c) Oil Industry, where the source of hydrogen is the corrosion reaction of steel with aqueous hydrogen sulfide solutions encountered either in the production of crude oil and natural gas (oil drilling and pipe line components) or in oil refining operations.

d) Aerospace Industry, where the components need both high strength and high toughness, hydrogen often plays an

adverse role. Because of the high strength, components such as bolts, landing gear, etc. are very susceptible to hydrogen embrittlement even though the hydrogen fugacity is very small.

In practice, the methods often proposed to prevent the hydrogen embrittlement ~~these~~ problems involve design modifications, changes in fabrication techniques, changes in material properties such as composition and heat treatment which involve changes in yield strength and microstructure of the material, and environmental control such as anodic or cathodic protection or lowering of the concentration of certain embrittling species such as H, H_2S, Cl, etc.

Basic Mechanisms

The fundamental mechanism of hydrogen-embrittlement is still not clear. Different basic mechanisms have been proposed. However, much controversy remains, particularly for embrittlement mechanisms where opposing models are still being supported.

Internal Pressure Theory

This theory first proposed by Zapffe and Sims[1] and later modified by others[2-4] asserts that embrittlement results from precipitation of molecular hydrogen at internal voids and the expansion of these voids by the development of high pressures within them and thus leading to the coalescence of the microvoids. This model is not adequate to explain the brittle fracture behavior in high strength steels exposed to low hydrogen pressure as observed by

Hancock and Johnson[5]. Brittle crack extension has been observed at hydrogen pressures well below one atmosphere.

Surface Free Energy Theory

Petch and Stables[6,7] suggested that hydrogen embrittlement could be due to the reduction of surface free energy (γ) by adsorbed hydrogen. Therefore, the nominal fracture stress, as given by the Griffith model[8] for a brittle crack in a purely elastic body, is lowered in proporation to $\gamma^{1/2}$. Hence a decrease in surface free energy would increase brittleness of the steel. The major drawback of this model is that it could not satisfactorily explain why other species, such as oxygen which adsorb more rapidly than hydrogen, are not equally potent embrittling agents. In fact, oxygen inhibits the crack growth in hydrogen, presumably by adsorbing at the crack tip and hence blocking it from hydrogen. Also, this model greatly underestimates the work of fracture. Crack growth in steel requires an energy which which is much greater than the surface energy; the excess energy is mostly utilized for plastic deformation at the crack tip.

Dislocation Mobility Model

Beacham[9], on the basis of his observations of decreasing microscopic plasticity and changes in the fracture mode with decreasing stress intensities during hydrogen-induced cracking, suggested that the role of hydrogen is simply to reduce the local stress required for dislocation motion. However, it has also been reported that both a

reduction and an enhancement of yielding at the crack tip occurred due to hydrogen[10].

Decohesion Theory

This theory suggests that the principal role of hydrogen is to lower the cohesive energy of the iron lattice. This concept was first introduced by Troiano[11] and is the basis of the theory proposed by Oriani[12-15]. According to this theory, hydrogen-induced crack growth occurs when the maximum elastic tensile stress, σ'_z, in the non-Hookean region of the crack tip equals $F_m(C')$, the maximum cohesive force between the atoms as reduced by the stress-induced, hydrogen concentration, given by the thermodynamic relation between chemical potential of an interstitial solute and the stress state[16]. In other words, the stress-controlled hydrogen-induced brittle fracture may be considered as a manifestation of diffusion of hydrogen to the regions of large hydrostatic tension ahead of the crack and concomitant lowering of the cohesive strength of the metal in proportion to the local hydrogen concentration. One important feature of this decohesion theory is that an immobile crack for which the above stress criterion is met under a given external hydrogen fugacity, is a situation of unstable chemical and mechanical equilibrium. Hence, at a given temperature and hydrogen fugacity, there exists a threshold stress intensity (K_{TH}) below which the crack will not grow. Similarly, at a given stress intensity and temperature, there exists a threshold hydrogen fugacity below which the crack will be stationary

indefinitely.

Threshold Stress Intensity

As stated in the decohesion model, for a given material, temperature, and hydrogen fugacity, there exists a threshold stress intensity level below which the crack growth rate in a hydrogen atmosphere is zero. At such a point, the crack can be considered to be in equilibrium. The existence of such a point would be of great interest both for design purposes and for fundamental studies. For design purposes the K_{TH} value, at a given strength level and hydrogen fugacity, indicates the highest stress level a cracked material can tolerate before crack extension occurs. Fundamentally, the study of K_{TH} value is of great importance in understanding the mechanism of hydrogen embrittlement which is controlled by both the state of stress and the diffusion of hydrogen from an external source to the highly stressed region ahead of the crack[11,12,16]. The threshold stress intensity K_{TH} for cracking in hydrogen can be determined by both falling K (constant displacement) and rising K methods. In the falling K method, K decreases as the crack grows. Eventually the growing crack arrests and reaches the K_{TH} point below which the crack velocity is essentially zero. The accuracy of the falling K technique depends mainly on the length of time of the tests, however; for the rising K technique both the loading rate and the sensitivity of the crack monitoring system govern the K_{TH} value.

Influence of Materials Properties and Other Environmental Controls on Hydrogen-Induced Cracking

As stated earlier, the remedies often proposed to reduce hydrogen embrittlement include a change in material properties, such as composition or yield strength, or a change in environment, such as minimising the hydrogen pressure or fugacity. A vast amount of research has been done on the effects of hydrogen pressure, yield strength, and different environments (such as H_2, H_2S, water vapour, etc.). Recently[17,18-21,22] a lot of attention has been given to the influence of composition of the steel on the hydrogen-induced cracking phenomenon.

Composition of the Material

It is often observed that quenched and tempered alloy steels have a tendency to fracture along prior austenite grain boundaries when exposed to certain environments e.g. hydrogen, hydorgen-sulfide, H_2SO_4 solution, or corrosive aqueous solutions e.g. NO_3^- or OH^- etc.[17,23,18-21,24]. As discussed earlier, this type of intergranular fracture mode is also associated with tempered martensite embrittlement which is believed[17,25-27,28-31] to be caused by the segregation of impurities to the grain boundaries, assisted by certain elements such as Mn, Si, etc. in the steel. Thus, the effect of grain-boundary composition on these environmentally-induced intergranular fracture problems may be an important factor to be considered. The effects of segregated impurities on hydrogen-assisted cracking (HAC)

on high-strength steel were first studied by Cabral et al.[18]. They tested smooth bars of a quenched and tempered 3 Ni-0.6 Cr-0.1 Mo-0.11 Cu-0.3C steel by static loading in tension in a 0.1 N H_2SO_4 solution and found that the threshold stress for cracking in this environment decreased significantly when the steel was given a temper-embrittlement treatment at 500°C for 48 hours. This drop in threshold stress was accompanied by a change in fracture mode from transgranular to completely intergranular failure.

Yoshino and McMahon[19] performed a similar study on a 5 pct Ni steel (HY 130), using statically loaded precracked edge-notched cantilever bend specimens in a similar H_2SO_4 solution (poisoned with As_2O_5) for both unembrittled and step cooled conditions. They found that the impurity-induced embrittlement had a profound effect on the resistance to crack growth in this hydrogen-producing environment. This is shown in Figure 1, which shows that the threshold K for crack growth dropped drastically when the steel was embrittled (step cooled). In the unembrittled condition the fracture mode changed from microvoid coalescence in air to transgranular fracture in the H_2SO_4 solution. Whereas, in the embrittled condition, the fracture mode was completely intergranular, both in air and the hydrogen-bearing environment. Later on, Briant et al.[20] and Mabuchi et al[22] studied the behavior of the same steel in a gaseous hydrogen atmosphere. Gaseous hydrogen was chosen to avoid uncertainties about surface-controlled reactions and the influence of variations

in the electrochemical conditions within the crack. They found that a small amount of impurity segregation produced a precipitous drop in the threshold stress intensity, K_{TH}, for cracking in hydrogen. The change in fracture mode was once again from transgranular at high K levels to predominantly intergranular fracture at low stress intensity levels. They identified the most potent embrittling element as Si, although P, Sn and perhaps N also contribued to the embrittlement to a smaller degree. In ultra-high strength steels, such as the 4340-type, which are tempered at relatively low temperatures, the impurity segregation which takes place during austenitization[17,27] is very low [17]. Nevertheless, it was found[17] to be sufficient to reduce significantly the threshold stress intensity K_{TH} needed for crack extension in the presence of hydrogen.

All these observations suggest that in commercial high strength ferritic steels, the brittle cracking in hydrogen occurs along prior austenite grain boundaries and that this is due to weakening of these boundaries by impurity segregation.

The technique most frequently applied to the study of hydrogen-assisted fracture is fractography. A wide diversity of fractographic responses to hydrogen have been reported in the literature depending on the stress intensity parameter K needed to produce cracking in hydrogen. It has been reported[17,19,20,22,32-33] that the fracture in hydrogen changes from quasi-cleavage to cleavage to intergranular as

the K decreases. However, recent studies have concluded that hydrogen promotes plastic instability[34,35] and causes fracture (presumably associated with the martensite lath structure[36,37]) by intense deformation by shear along slip bands. Recently, Takeda and McMahon[38] by systematic variation of the composition of the HY130 steel (while maintaining the same basic microstructure and strength) observed both the above strain-controlled shear fracture and the stress-controlled intergranular brittle fracture in the same material at a fixed hydrogen pressure and temperature. This is shown in Figure 2. They[38] found that for a Mn and Si-free steel, the cracking in hydrogen occurs on the two planes of maximum shear stress ahead of the main crack resulting in branching at the crack tip. They associated this type of fracture with the "sweep in" of hydrogen by the dislocations on these shear planes resulting in local build-up hydrogen and essentially producing decohesion along shear bands. On the other hand, in a commercial steel (where Mn, Si, and other residual elements such as Sn, P, etc., are present), the fracture mode was once again brittle and intergranular.

Strength of the Material

It is now well recognized that the higher strength materials are more susceptible to hydrogen embrittlement[32, 39-43]. It is generally observed that at lower strength levels no slow crack growth in hydrogen occurs, whereas at higher strength levels K_{TH} for cracking in hydrogen drops

as the strength level of the material increases. Sandoz [40,41] studied the effects of hydrogen on K_{TH} in a commercial-purity 4340 steel and based, on his observations of similar fracture modes at equal values of threshold stress intensities, he concluded that the effects of hydrogen were fundamentally the same whether the hydrogen originated from the gas, from stress corrosion, or from electrolytic charging during or prior to testing. He also concluded that the fracture mode in the vicinity of K_{TH} was governed mainly by the hydrogen concentration and yield strength rather than the source of hydrogen. Nelson and Williams[43] studied the hydrogen-induced slow crack growth in a AISI 4130 low alloy steel in gaseous hydrogen as a function of applied stress intensity, K, at various strength levels. They observed that both stage I and stage II growth were influenced by variations in strength level and that K_I, which essentially represented the threshold stress intensity, varied proportional to $\sigma_y^{-5.2}$ and $\sigma_u^{-3.6}$, where σ_y and σ_u yield strength and U.T.S. respectively. Later on, Gerberich and Chen[42], using samples precharged with hydrogen prior to testing, correlated the threshold stress intensity required to cause hydrogen embrittlement with the yield strength of the material through the fracture mechanics approach. They derived a quantitative relation between between stress intensity, yield strength, temperature, hydrogen concentration and specimen thickness using the decohesion criterion proposed by Oriani and Josephic[12-15].

The first drawback of their [42] approach is that they used a precharged sample and so it would be extremely difficult to assess the free body (i.e. unstressed lattice) equilibrium concentration of hydrogen after cathodic charging. Secondly, while considering the stress gradient ahead of the crack tip which involves both plastic and elastic stresses, they calculated the triaxial tension by using Hill's slip-line field equations for plane strain. This estimation is suitable for notched specimens where both the magnitude and position of the maximum tensile stress change with the extent of plastic deformation. However, for a precracked specimen, at a particular strength level, the magnitude of the maximum principal tensile stress (σ_{22}) is fixed, and only the stress gradient changes with plastic deformation. Even so, from their experimental observations they clearly showed that the threshold stress intensity decreased as the yield strength of the material increased.

It may be noted that all the observations mentioned above on the dependency of K_{TH} on yield strength involve commercial-purity high strength steels. This problem was never approached from the impurity point of view until recently, when Viswanathan and Hudak[32] studied the effect of impurities and strength levels on hydrogen-induced cracking in an H_2S environment. They found a reduction in the K_{ISCC} in H_2S when the steel was given a prior temper embrittlement treatment. They also found that this effect was pronounced at low and intermediate strength

levels and the amount of intergranular fracture was uniquely related to K_{ISCC}.

Hydrogen Pressure or Fugacity

In general, it has been observed that the K_{TH} for cracking in hydrogen decreases as the hydrogen pressure or hydrogen fugacity increases[14,43-45]. However, a wide variation of the functional relationship between K_{TH} and P_{H_2} for different materials exists in the literature. Clark[44] studied the effect of H_2 and H_2S pressure on of a commercial 4340 type steel of 180 ksi yield strength. He found that gas pressures ranging from 5 psig(0.14 MPa) to 100 psig (0.79 MPa) did not have a significant effect on the room temperature K_{TH} when tested in an H_2S environment. However, the gas pressure did show a significant effect on K_{TH} when tested in dry hydrogen as shown in Figure 3. Assuming that the fundamental mechanism of hydrogen embrittlement are essentially identical in both H_2 and H_2S gases, for some reason the H_2S gas more easily supplies the atomic hydrogen required to do the damage. The ability of H_2S to make hydrogen atoms readily available was shown by Kemball[46]. On the basis of energetics alone, the accelerating effect of H_2S is reasonable. The H-H bond energy is 434 KJ/mole and H-S is 346 KJ/mole, so, hydrogen atoms are available from H_2S at a lower energy than from H_2. Also, because of the poisoning effect, H_2S retards the recombination of atomic hydrogen into molecular hydrogen[47]. These reasons also explain

the faster crack growth rate in H_2S than H_2 although the K_{TH} remains the same[44]. This is simply because the crack growth rate is mainly controlled by the kinetics of the hydrogen transport processes. Clark[44] found that K_{TH} in hydrogen gas decreased linearly with log P_{H_2}. A similar linear relationship was also observed by Oriani et al.[14] and Gerberich et al[45]. It was also observed that for a given hydrogen pressure, the lower strength steels were generally more sensitive to variations in pressure than the higher strength steels.

Temperature

In general, K_{TH} increases with increasing temperature. However, the sensitivity to changes in temperature varies widely from steel to steel. Most of the investigations on the effect of temperature involved the study of kinetics of the hydrogen transport phenomenon on the crack growth rate in a hydrogen environment[48-52]. Fundamentally, the temperature controls the rate at which hydrogen can diffuse through the iron lattice to the region of maximum hydrostatic tension. Temperature also influences the tendency of the gas molecules to be adsorbed on the free surface; this can result in a precipitous drop in crack growth rate with an increase in temperature. The temperature also influences the yield strength and ductility of the steel which in turn controls the local hydrogen concentration for crack growth; of course, this effect is very small in a high strength steel.

SCOPE OF THE PRESENT INVESTIGATION

Hydrogen-Induced Cracking

As proposed by Troiano[11] and later modified by Oriani[12-15], the phenomenon of hydrogen-induced brittle fracture is a manifestation of the reduction of the strength of interatomic bonding in the Fe-lattice. In this sense, it can be closely related to the effects of metalloid elements segregated to the grain boundaries which are known to produce the same effect.

Most of the proposals in the literature regarding the mechanism of hydrogen embrittlement (HE) are based on work done on commercial steels only. Since, it is often observed that quenched and tempered alloy steels have a tendency to fracture along prior austenite grain boundaries when exposed to hydrogen (similar to the fracture mode associated with tempered martensite embrittlement), it was felt that knowledge of the mechanism for HE will be incomplete without considering the interaction of segregated metalloid elements and hydrogen.

In this work, a connection was made between tempered martensite embrittlement and hydrogen-induced cracking in high strength steels. By a systematic variation of the composition of the steel, while maintaining the same basic microstructure, the combined impurity and hydrogen effects in 4340-type steels were studied for different strength levels and for different hydrogen pressures. In the course of the present work, the following key questions were

addressed:

1. What are the most important impurity elements responsible in promoting intergranular cracking in a hydrogen atmosphere at low stress intensity levels?
2. What are their relative potencies and how much of their segregation is necessary in promoting this embrittlement?
3. Is there a relationship between TME and HE; if so what is the nature of such a relationship, i.e., additive or synergistic?
4. What are the alloying elements that promote this embrittlement?
5. What is the influence of yield strength and hydrogen pressure on this embrittlement and what significant role do the impurities play at these pressures and yield strength levels?
6. Is there a unique relationship between local hydrogen concentration and threshold stress intensity K_{TH} for cracking in hydrogen; if so what is the role of impurities in such a relationship?
7. Finally, and not the least, how can these problems be eliminated?

EXPERIMENTAL PROCEDURE

See PART I.

EXPERIMENTAL RESULTS

Fracture Behavior in Hydrogen

The behavior of these steels in a gaseous hydrogen atmosphere was found to be extremely sensitive to small changes in composition, yield strength, and hydrogen pressure. In order to get a clear picture of these effects, a large number of experiments were done in a hydrogen atmosphere and also in the absence of hydrogen.

The crack growth in hydrogen in bolt-loaded WOL specimens was monitored by recording the drop in load on the tup (load cell) as a function of time. An analog-to-digital converter was used and the millivolt output was recorded by a teletype. In the early (rapid) stages of crack growth the readings were taken every three seconds; the time interval was increased as the crack slowed down. Figure 4 shows an example of an a vs. t curve for steel 840 at 23°C and 1 psig. (0.11 MPa) hydrogen pressure. In general, the crack length appeared to vary smoothly with time, as opposed to discontinuous, stepwise crack growth observed by Briant et al in a lower strength HY 130 steel. The crack growth rates were determined by taking the slopes of the approximately linear segments of the a vs. t plot shown in Figure 4. The conventional log V (= log $\frac{da}{dt}$) vs. K plot is shown in Figure 5 for several steels having a yield strength of 1450 MPa.

Effects of Composition

In a previous study[17] of several commercial and laboratory heats of 4340-type steel it was shown that the threshold stress intensity (K_{TH}) required for crack extension in 0.11 MPa H_2 at 23°C can vary over a wide range, depending on the tendency for intergranular fracture, which in turn depends on the composition of the steel. That research has now been extended by the addition of more laboratory heats. These heats were designed to reveal the effects of increasing the Mn content in the presence of low Si and increasing the Si content in the presence of low Mn. The purpose was to clarify the respective roles of these elements in promoting intergranular cracking in a hydrogen atmosphere at low stress intensity levels. If we plot the measured K_{TH} values of all the steels examined so far (with yield stress = 210 ksi, 1448 MPa) vs. a composition parameter (Mn + 0.5 Si + S + P) which lumps the bulk concentrations of Mn, Si, S, P together in the appropriate way (found by trial and error), we can fit all the results on one curve, and is shown in Figure 6. It is apparent that an increase in the Mn and/or Si concentration in the presence of small amounts of S and P causes a drastic reduction in K_{TH} value. Note that these are for steels with P in the range 30-140 ppm and S in the range 30-160 ppm. This reduction in K_{TH} corresponds to an increase in the amount of intergranular fracture from <20% to almost 100%

as shown in Figure 7. Hence these results reflect the tendency of the segregation of P and S (presumably by Mn and Si) on the prior austenite grain boundaries and their interaction with the hydrogen. The evidence for segregation of P and S (from Auger analysis) has already been presented in Part I Report.

Obviously, one would be interested to know the magnitude of the contribution of hydrogen alone to K_{TH} in these steels. Figure 8 shows how K_{IC} in air and K_{TH} for cracking in hydrogen varies with the same composition parameter that was used before. At low values of the parameter, hydrogen has almost no effect on the K required for detectable crack extension. However, from SEM observations, it has been found that the hydrogen-induced cracking mode in the "pure" steel includes what may be transgranular fracture in addition to separation of some type of interface, presumably between martensite laths, in contrast with the rupture which occurs in air. As the composition parameter increases, we observe increasing amounts of cracking along prior austenite grain boundaries and hence the K_{TH} value drops well below K_{IC}. The increasing tendency in K_{IC} at higher values of the parameter, is presumably due to the effect of the higher Mn content. Figure 9 shows the results of the scanning electron microscopy of the fracture surfaces at three different K_{TH} levels, and Figure 10 shows the ultimate relationship between K_{TH} and the corresponding percent

intergranular fracture for these steels with varying amounts of Mn, Si, P and S. From these results it was concluded that the effect of hydrogen on K_{TH} is largely due to impurity segregation, and the principal effect of the composition parameter is to control the amount of P and S segregated to the grain goundaries during austenitization, and thus the strength of these boundaries.

Effects of Yield Strength

Until now all the results presented referred to a particular yield strength (210 ksi, 1450 MPa). We postulate that the cohesion of steel can be lowered by an increase in concentration of either hydrogen or metalloid impurities. Hydrogen segregates to regions of hydrostatic tension even at room temperature (because of its extraordinary high mobility in bcc Fe), and the attainable hydrostatic tension depends very much on the yield strength of the material. It has long been recognized that higher strength steels are more susceptible to hydrogen embrittlement[32,39,42-43]. In the present study, an investigation was made of the combined impurity and hydrogen effects in the yield strength range 1140 to 1900 MPa (165 to 270 ksi).

High-Purity 4340-type Steels

Figure 11 shows the variation of K_{TH} in 0.11 MPa H_2 at 23°C with the yield strength for the "pure" steel B7. At low strength levels, no substantial crack growth is observed. At higher strength levels the K_{TH} value decreases

gradually with increasing strength until it reaches a value around 40 ksi $\sqrt{in}$ (44 MPa$\sqrt{m}$). This drop in K_{TH} value corresponds to an increase in the amount of intergranular fracture, as shown in Figure 12. Thus, even in the pure steel where the segregation of impurities to the grain boundaries is very small, an increase in yield strength of the material leads to an increase in the amount of intergranular fracture. It is apparent from the K_{IC} data included in Figure 11 that hydrogen has almost no effect on the K required for detectable crack extension at lower values of the yield strength. However, from the SEM observations made on the fracture surface it does produce a change in the fracture mode from rupture in air to some sort of transgranular cracking and/or interface decohesion, apparently in and between martensite laths[34-38]. Figure 13 shows the scanning electron micrographs of the fracture surfaces of this steel at three different strength levels. The fracture mode changes gradually to predominantly intergranular fracture as the yield strength increases.

Figure 14 shows the relationship between K_{TH} in hydrogen and the corresponding intergranular fracture for steel B7 for different yield strength levels.

Commercial 4340-type Steels

Effect of Mn and Si:

It has already been demonstrated in the previous sections that both Mn and Si have profound effects in

promoting tempered martensite embrittlement and hydrogen embrittlement, presumably by promoting segregation of P and S to the prior austenite grain boundaries. The effects were demonstrated mostly at a particular strength level. To elucidate their importance at different strength levels, K_{TH} measurements in a 0.11 MPa H_2 at 23°C were done on the Mn + Si doped pure steel B6. Figure 15 shows the variation of K_{TH} with yield strength for steels B6 compared with B7. When Mn and Si were added to get steel B6, the K_{TH} value dropped well below that of steel B7 at all strength levels. The difference becomes especially significant at intermediate strength levels. Two points are to be noted here:

First, when the grain boundaries are highly contaminated as in the case of steel B6, the brittle fracture in hydrogen occurs at relatively lower strength levels even though the attainable hydrostatic tension is small, whereas in case of steel B7, the grain boundaries are less contaminated and hence the brittle fracture occurs only at relatively higher yield strength levels.

Secondly, the difference in the K_{TH} value through the entire yield strength range can be attributed mainly to the difference in segregation of impurities between these steels.

In order to study the contribution of hydrogen in a commercial steel, tests were done in hydrogen and also in the absence of hydrogen. Figures 16 and 17 show how K_{IC}

in air and K_{TH} for cracking in hydrogen vary with the yield strength for a vacuum melted lab heat B6 and a commercial air-melted heat B2. It may be seen that when the grain boundaries are highly contaminated, the effect of hydrogen tends to be much more pronounced and hence the K_{TH} for cracking in hydrogen drops well below K_{IC}. At the lower strength levels (170 ksi, 1170 MPa), since K_{IC} in air and K_{TH} in hydrogen tend to converge, hydrogen has little effect on the K required for crack extension, but once again like the pure steel B7 (Figure 13), it does produce a change in fracture mode from complete rupture in air to the other H_2-induced mode, described earlier. Figure 18 shows a scanning electron micrograph of the fracture surface for steel B6 at low strength level. The fracture appears to be mostly interlath, with a bit of rupture. As the yield strength of the material increased, the fracture mode changed gradually from inter-lath to predominantly intergranular as shown in Figure 13 for pure steel B7.

Figures 19a and 19b show the drop in load and corresponding increase in the crack length for an advancing cracking in a 0.11 MPa H_2 at 23°C for two different strength levels (170 ksi, 1170 MPa and 270 ksi, 1860 MPa) respectively. Several points are to be noted here:
In case of the low-strength material (Figure 19a):

1. We need much higher load (or K) for the crack to propagate.

2. The crack traversed a very small distance, an order of magnitude less than the high strength steel.
3. The crack propagated very slowly in spite of the fact that the total distance it traversed was very small.
4. The actual crack length, measured from the fractured sample, is smaller than that calculated from the compliance curve. This is presumably because of crack branching[35,38] at the tip of main crack.

The cracking occurred on the two planes of maximum shear stress ahead of the main crack at the low yield strength levels, as shown in Figure 20 for two steels B6 and B7. In both cases, the cracking did not occur along prior austenite grain boundaries, but presumably along the martensite lath boundaries, and perhaps partly across laths, as shown in Figures 13a and 18. Presumably, this cracking phenomenon is connected with the process of plastic shear at the tip of the main crack. The details of this type of cracking phenomenon are described elsewhere[38].

In the case of the high-strength material (Figure 19b):

1. The crack started at a relatively low load.
2. The crack traversed a long distance.
3. The crack-growth rate was much higher than the low yield strength material.

4. The cracking occurred on a single plane (by Mode I) and was thus presumably a stress-controlled, brittle decohesion along prior austenite grain boundaries, as observed in a typical commercial steel where the grain boundaries are weakend by various metalloid impurities.

Effects of Hydrogen Fugacity or Pressure

The hydrogen pressure or fugacity has profound effect on both the equilibrium value of K_{TH} and the rate at which the hydrogen-induced cracking occurs[14,43-45,50]. Figure 21 shows the effect of hydrogen pressure on K_{TH} for cracking in hydrogen for the pure steel B7 and the commercial steel B2. The K_{TH} value decreases for both steels as the pressure of hydrogen increases. It may be seen that for a particular K_{TH} level (as for example ~40 ksi$\sqrt{in}$, 44 MPa$\sqrt{m}$), a very small pressure of hydrogen is needed for crack extension in the case of the commercial steel B2. However, when the grain boundaries are less contaminated (steel B7), we need 8 to 10 times more pressure of hydrogen for cracking. When the yield strength of the material was increased from 210 ksi (1450 MPa) to 250 ksi (1725 MPa), the pressure of hydrogen to produce brittle cracking dropped by about half in the case of steel B7.

The hydrogen dissolved in the iron lattice exists in the dissociated form and occupies the interstitial posi-

tions, as well as traps, such as dislocations and grain boundaries; the equilibrium solubility of hydrogen (C_o) in an unstressed α-lattice can be calculated from Sievert's law and is given by the expression(53)

$$C_o = 3.7\ p^{1/2} \exp\left(\frac{-6500}{RT}\right)$$

where C_o is expressed in cm^3 H_2 (STP)/cm^3Fe, p is pressure in atmosphere and T in degrees Kelvin with heat of solution as 6500 $\pm$ 300 cals/g.atom. Figure 22 shows how the calculated value of C_o was related to the K_{TH} for the same two steels. The behavior is similar (as expected) to that of the dependence with hydrogen pressure. Assuming C_o to be constant for these steels at a particular hydrogen pressure (because the microstructure remains the same for both these steels), it may be seen that pure steel B7 shows much higher K_{TH} value than the commercial steel B2 for a particular strength level (in this case 210 ksi, 1450 MPa). The curves tend to converge together at higher C_o values.

To account for the effect of hydrogen, we assume that the reduction in cohesive strength by hydrogen is proportional to the local hydrogen concentration C_H. This local hydrogen concentration can be calculated from the thermodynamic expression given by Li et al.(16). Of course, to calculate C_H, one must know the maximum hydrostatic tension ahead of the crack tip which can be calculated in terms of the yield strength of the material using the elastic-plastic stress analysis of Rice and

Johnson[54]. An increase in hydrogen pressure or fugacity (i.e. C_o) and/or an increase in the yield strength of the material, will increase the local hydrogen concentration C_H. As far as present experimental conditions are concerned, it appears that the threshold stress intensity value K_{TH} for cracking in hydrogen has a unique relation with calculated value of C_H for various combinations of hydrogen pressure and yield strength of the material. This is shown in Figure 23 for the pure steel B7 and the commercial steel B2. We get two different curves; the difference between them presumably shows the effects of the metalloid impurities. It may be seen from this figure that for particular values of C_H, the K_{TH} value for commercial steel B2 drops well below that of the pure steel B7.

DISCUSSION

Hydrogen-Induced Cracking

When hydrogen is absorbed by a steel under stress, it can affect both the plastic behavior and fracture properties. The most important effect of the absorbed hyrogen is that it reduces the cohesive strength, or interatomic bonding, of the iron lattice. In this sense, it is analogous to the effects of metalloid elements segregated to grain boundaries. As discussed in Part I, the segregation of these impurity elements causes a reduction in the ideal work of fracture γ, which in turn causes a larger reduction in the plastic work γ_p and thus large embrittlement effects. Such a reduction in γ can apparently also be caused by the absorption of hydrogen. The main concern is how, or whether, hydrogen and impurities interact with each other with respect to intergranular decohesion. To study this one has to know the variation of γ with hydrogen concentration C_H. However, at present time, there is no way to measure this relationship directly.

On the macroscopic scale, the threshold stress intensity K_{TH} for crack extension in a hydrogen atmosphere can be assumed to characterize in some way the degree of reduction of cohesion along grain boundaries. By using the falling K method at a given temperature and hydrogen fugacity, the propagating crack under constant displacement has been allowed to come to rest at a certain value of

K. Therefore, this K_{TH} value is be assumed to be an equilibrium situation and to be related to the equilibrium hydrogen concentration C_H.

It is concluded that hydrogen (H) when dissolved in iron and steel, has been observed to produce the following phenomena:

1. Brittle cracking by the decohesion of prior austenite grain boundaries which are already weakened by the segregation of impurity elements (17,19-20,22,32,55-56). This type of hydrogen induced fracture is a stress-controlled brittle decohesion and comprises Mode I cracking.
2. Glide-plane decohesion in iron single and polycrystals(21,36,57,58,59) and in martensitic or bainitic steels along/across laths or plates(37,38). This type of cracking phenomenon is characterized by apparently quasi-brittle cracking along {110} or {112} planes and is presumably due to the local build-up of hydrogen in heavily dislocated shear bands resulting from the "sweep-in" of dislocation core-trapped hydrogen(36,37,58). This is a strain-controlled fracture mode and occurs by Mode II cracking. A model for this fracture mechanism is given elsewhere(38).
3. Enhancement of void formation and subsequent rupture due to trapping and build-up of hydrogen

at particle-matrix interfaces[60].

Brittle Intergranular Fracture

Hydrogen-induced brittle fracture of high-strength steels is one of the most pervasive and damaging modes of failure of structural materials. Its importance is growing with the increasing use of steels with yield strength above ~700 MPa. As demonstrated by the experimental results in the previous section, this type of fracture occurs by brittle separation along prior austenite grain boundaries and is a stress-controlled brittle decohesion of the same type that occurs when metalloid elements embrittle grain boundaries without the action of hydrogen. Here, it has been demonstrated how hydrogen acts in promoting fracture, and how it interacts with the compositional and microstructural factors, through the yield strength of the material.

The metallurgical factors which control the tendency for hydrogen-induced brittle intergranular cracking are:

1. Material Properties Variables, such as composition and yield strength. Compositional changes control the degree of embrittlement of the grain boundaries, and the yield strength changes control the capacity to absorb hydrogen and also the stress distribution ahead of the main crack.
2. Environmental Variables such as hydrogen fugacity. The hydrogen fugacity, of course, depends upon whether hydrogen is available in the gaseous form

or is introduced by means of cathodic charging and this controls the hydrogen concentration in the matrix.

With Oriani[12-16], and Troiano[11,61] before him, the phenomenon of hydrogen-induced brittle crack propagation utilizes a stress criterion, postulating that the dissolved hydrogen in iron at a sufficiently large concentration decreases the cohesive strength of the metal and the latter is a monotonically decreasing function of the hydrogen concentration. Hydrogen tends to collect at the regions of hydrostatic tension ahead of the crack tip even at room temperature (because of its extraordinary high mobility in b.c.c. iron), whereas surface-active impurities segregate to the grain boundaries only at high temperature (since they are substitutional elements and diffuse slowly). The equilibrium maximum hydrogen concentration C_H in the crack tip region can be calculated from the thermodynamic expression derived by Li et al.[16]

$$C_H = C_o \exp\left(\frac{\theta\Omega}{RT}\right) \qquad (1)$$

where, C_o is the equilibrium hydrogen concentration in the unstressed lattice, is the maximum hydrostatic tension and is given by $\theta = \frac{\sigma_1+\sigma_2+\sigma_3}{3}$, R is the gas constant and T is the temperature expressed in degrees Kelvin. Now, according to Sievert's law, $C_o = k(P_{H_2})^{1/2}$ and the value of θ, in principle, can be expressed in terms of the yield strength

of the material using the elastic-plastic stress analysis of Rice and Johnson[54]. This can be expressed as $\theta = \alpha \sigma_y$. Therefore, the equation (1) can be written as,

$$C_H = k (P_{H_2})^{1/2} \exp\left(\frac{\alpha \sigma_Y \Omega}{RT}\right) \qquad (2)$$

where, k is the Sievert's law coefficient and α is a constant $\simeq$ 2.9 for a non-strain-hardening material.

Therefore, at a particular yield strength and at a given hydrogen fugacity, the equilibrium hydrogen concentration can be estimated for a particular steel. A similar approach, based on Oriani's decohesion model, has been also carried out by Gerberich and Chen[42]. Using pre-charged samples, they tried to derive a quantitative relationship between the threshold stress intensity K_{TH}, the hydrogen concentration, and the yield strength of the material.

Strictly speaking, the calculation of the equilibrium hydrogen concentration is done in a continuum macroscopic sense and is based totally on thermodynamic considerations. Therefore, this represents, the bulk hydrogen concentration near the crack tip region. However, in the microscopic sense, one must consider those phenomena which might enhance the local hydrogen concentration. These could be as follows: a) Hydrogen interaction with dislocations. It is now generally accepted that hydrogen when dissolved in iron, is strongly attracted to the

cores of dislocations and the core-trapped hydrogen concentration is quite high at room temperature[62]. The local hydrogen concentration at the grain boundaries might increase due to the pile-up of these dislocations at the grain boundaries. b) The grain boundary, itself, may be the sink for hydrogen accumulation. As observed by several authors[63,64] using a tritium autoradiography technique, it has been shown that in Armco iron and in maraging steel of hydrogen is trapped at prior austenite grain boundaries. Tritium was also observed at sub-grain boundries, grain boundary carbide/matrix interfaces, and at martensite plate boundaries. However, the density of silver filaments on the autoradiographs was higher in the prior austenite grain boundaries than in the martensite plate boundaries. c) The solubility of hydrogen in iron may vary with the addition of alloying elements as illustrated by Oriani[53] and Weinstein and Elliott[65] in the case of liquid iron.

From the present investigation, it is evident that both hydrogen and metalloid impurities (such as P and S) induce intergranular embrittlement. The impurities which were observed to cause tempered martensite embrittlement also played a deleterious role in hydrogen. In these ultra-high strength steels, which are tempered at relatively low temperatures, the impurity segregation takes place (as discussed in Part I) during austenitization[27], and is therefore of quite low concentration. Nevertheless,

it is sufficient to reduce significantly the threshold stress intensity K_{TH} needed for crack extension in the presence of hydrogen (Figure 6) and an increase in the amount of decohesion along prior austenite grain boundaries (Figure 7). Although the general form of the composition parameter used in this study can be rationalized qualitatively from thermodynamic considerations, as discussed in the previous section, there is no fundamental basis for its specific form; at present it is purely empirical. However, it is a rational and useful guide for the future improvement of commercial grade steels.

The physical importance of the variation of K_{TH} with solute segregation which involves the interaction of both impurity elements and hydrogen, can be explained by the model for stress gradient control of brittle fracture developed by Kameda[66], in conjunction with the newly developed microscopic theory of brittle fracture[67]. The basic idea of the model[66] is to describe how the local stress intensity (k) at the microcrack tip is influenced by the steep stress field due to the precrack, on the assumption that the nucleated microcrack of some size lies in the maximum stress region. As described in the previous section, the microcrack which is generally nucleated at an intergranular second phase particle (inclusion or carbide) will propagate unstably only when the energy criterion is satisfied, i.e. when the elastic strain energy release rate at the microcrack tip exceeds

the sum of the fracture energies γ and γ_p[67]. By estimating k_{IC} from the measurements of σ^* vs. solute segregation on the notch bend tests and by measuring the corresponding value of K_{IC} with respect to intergranular solute coverage, correlation between k and K has been produced[66]. This is shown in Figure 24. It may be seen from the figure that at higher values of K_{IC}, a small reduction in k_{IC} due to solute segregation causes a large reduction in K_{IC}. This is analogous to the behavior in hydrogen, as depicted in Figure 6, where we find a large drop in K_{TH} value with a slight increase in the composition parameter which, of course, reflects the tendency of solute segregation on the prior austenite grain boundaries. At lower values of K_{IC}, a large decrease in γ, or k_{IC}, leads to a relatively small reduction in K_{IC}. This is reflected in Figure 6, where the K_{TH} value essentially remains constant or changes slightly with increases in the composition parameter at higher values.

From all these foregoing discussions, it seems reasonable to correlate somehow both the impurities and the hydrogen, with the threshold stress intensity K_{TH} which characterizes the degree of intergranular embrittlement in hydrogen (Figure 10). As shown previously in Figure 23, in these 4340-type steels with yield strengths in the range 1200 to 1900 MPa, and within the present experimental conditions, K_{TH} is a monotonically decreasing function of the calculated equilibrium hydrogen concentration C_H.

Each point on the curves in Fig. 23 was obtained by varying the yield strength and hydrogen pressure independently. The upper curve was obtained for a high purity NiMoVC steel of the 4340 composition, but without any Mn or Si, both of which promote intergranular segregation of residual P and S. The lower curve is for a commercial purity 4340 steel. This illustrates two important points as discussed before: First, this supports the idea previously proposed by Troiano[11,61], Oriani[12-16] and others[42] that the hydrogen-induced brittle fracture occurs by stress-induced concentration of hydrogen, which acts to lower the cohesive strength of metal and the latter is a monotonically decreasing function of hydrogen concentration. Secondly, the segregated impurities such as P and S have a dominant role in promoting this type of brittle intergranular embrittlement in hydrogen at low stess intensity levels, as proposed by other investigators[17,19,20,32].

We cannot say yet definitively whether the hydrogen and impurity effect is simply additive or is synergistic, because such a prediction needs an experiment in which one can determine the local values of stress, hydrogen concentration, and impurity concentration at the initiation of brittle cracking, and the systematic variation of these factors. However, an insight into this behavior can be obtained from the Figure 25. Here, K_{TH} values in hydrogen are plotted against a parameter which includes

the calculated equilibrium hydrogen concentration and the composition parameter that has been used previously. Each point on the curve was obtained by varying independently the composition, yield strength and hydrogen pressure. We get a unique curve for all the steels that have been studied in the present investigation. Three important conclusions can be made from this figure: First, both hydrogen and metalloid impurity elements indeed reduce intergranular cohesive strength of the metal and this is reflected by an increase in the amount of intergranular fracture as shown in the next Figure 26. Secondly, hydrogen has a tremendous effect on decohesion, and only very small impurity segregation is more than enough to cause this decohesion. Thirdly, the curve in Fig. 25 is consistent with the idea that hydrogen and impurities interact additively.

Plasticity-Related Hydrogen-Induced Fracture

As stated earlier in the previous section, at low yield strength levels, the fracture mode is completely transgranular in both pure and commercial steels (Figures 13a, 18) and is different from so-called quasi-cleavage type fracture. This latter fracture mode, which is usually observed at high stress intensity levels, is intimately related to the plastic flow at the tip of the precrack[38]. The fracture actually occurs along the two planes of maximum shear stress ahead of the main crack (Figure 20) and thus proceeds by Mode II fracture.

Since, the precrack is effectively branched when this plasticity-induced hydrogen fracture occurs, obviously the threshold stress intensity measurement does not represent pure Mode I loading. In addition, these cracks are not detected by the usual compliance calibration method (by bolt-and-tup arrangement) until they are fairly well developed. Recently Takeda and McMahon[38] have proposed a mechanism related to this type of fracture which is analogous to the behavior of Zn at low temperature as demonstrated by Gilman[68] in an asymmetrical zinc bicrystal. They[38] have suggested that this is due to the transport of hydrogen by the cores of dislocations emitted at the tip of the main crack because of severe plastic deformation. These dislocations moving away from the main crack, carry hydrogen with them and accumulate it along the slip band. When the accumulation becomes sufficient, it results in glide-plane decohesion as the edge dislocations are blocked at barriers such as carbides formed in the lath boundaries. This results in "lath"-type fracture as shown in Figures 13a, 18. Similar type of fracture has been also reported by others[34-37,57]. The trapped hydrogen also enhances screw dislocation mobility, presumably by reducing the Peierls stress and inhibiting cross slip and thereby promotes crack tip plasticity as it does in iron at low temperature[69].

Finally, it appears that there are three independent variables that can be manipulated to control the suscep-

tibility to hydrogen-induced cracking: the hydrogen pressure or fugacity, the yield strength of the steel, and the purity of the grain boundaries of the steel. For a given hydrogen fugacity, the strength of the steel that can be safely tolerated depends directly on the purity of the grain boundaries. The most potent impurity elements that are found to reduce the resistance to hydrogen susceptibility are P and S and presumably the alloying elements such as Mn and/or Si promote the segregation of these impurity elements. In this context, it must be mentioned here that the threshold stress intensity values in an H_2S environment on a similar 4340-type steels (pure and impure) observed by Viswanathan and Hudak[32] are relatively smaller than that observed in this study. This is presumably due to two factors: First, their so called "pure" steel has commercial levels of Mn and Si with trace amounts of P and S. Secondly, unlike this study (in hydrogen gas environment), their observations have been done in an H_2S environment. Therefore, the hydrogen fugacity is much higher than the present study.

SUMMARY AND CONCLUSIONS

Hydrogen Embrittlement

1. Hydrogen-induced fracture in high strength steels of commerical purity occurs by brittle separation along prior austenite grain boundarie, and this is a stress-controlled, brittle decohesion of the same type that

occurs when metalloid elements embrittle grain boundaries without the action of hydrogen.

2. The impurities (P and S) which are observed to cause tempered martensite embrittlement, also play a deleterious role in hydrogen-induced cracking. In these ultra-high strength steels, the crack-tip stress level and the concomitant stress-induced equilibrium hydrogen concentration are so high that very small amounts of segregated P and/or S are enough to lower drastically the H-cracking resistance along grain boundaries.
3. Although we cannot say yet definitely whether the hydrogen and impurity effect is simply additive or synergistic, the results obtained here are consistent with an additive effect.
4. Increasing either the yield strength or the hydrogen pressure or fugacity increases the susceptibility to hydrogen-induced cracking. For a given hydrogen fugacity (as determined by the environment), the strength of the steel that can be safely used depends upon the purity of the grain boundaries.
5. When the amount of impurity segregation on the grain boundaries is high (as in case of commercial steels), we need less hydrogen for brittle cracking. Whereas, when the grain boundaries are less contaminated more hydrogen is necessary for crack extension in hydrogen.

REFERENCES

1. C. Zapffe, and C. Sims; Trans AIME, Vol. 145, 1941, p. 225.
2. F. J. de Kazinczy; J. Iron Steel Inst., 1945, Vo. 177, p. 85.
3. F. Garofalo, Y. T. Chou, and R. Ambegaokar; Acta Met., 1960, Vol. 8, p. 504.
4. A. S. Tetelman, W. D. Robertson; Acta Met., Vol. 11, 1963, p. 415.
5. G. G. Hancock, and H. H. Johnson; Trans. Metall. Soc. AIME, Vol. 236, 1966, p. 513.
6. N. J. Petch, and P. Stables, Nature, Vol. 169, 1952, p. 842.
7. N. J. Petch; Phil. Mag., Vol. 1, 1956, p. 331.
8. A. A. Griffith; Phil. Trans. Roy. Soc. (London) Vol. A221, 1920, p. 163.
9. C. D. Beacham; Met. Trans., Vol. 3, 1972, p. 437.
10. H. Kimura, H. Matsui, and T. Kimura; Proc. Int. Symp. on "Hydrogen in Metals", Minakami, Japan, 1979; Trans. JIM, Vol. 21, 1980, p. 533.
11. A. R. Troiano; Trans. ASM, Vol. 52, 1960, p. 54.
12. R. A. Oriani; Ber der Bunsen-Geselsch. f. phys. Chem. Vol. 76, 1972, p. 848.
13. R. A. Oriani; Stress Corrosion and Hydrogen Embrittlement of Iron-Based Alloys, NACE, Houston, Texas, 1975.
14. R. A. Oriani, and P. H. Josephic; Acta. Met., Vol. 22, 1974, p. 1065.
15. R. A. Oriani, and P. H. Josephic; Acta. Met., Vol. 25, 1977, p. 979.
16. J. C. M. Li, R. A. Oriani, and L. S. Darken; Z. Phy. Chem. Frankfurt, 1966, Vol. 49, p. 271.
17. S. K. Banerji, C. J. McMahon, Jr., and H. C. Feng; Met. Trans., Vol. 9A, 1978, p. 237.
18. U. Q. Cabral, A. Hache, and A. Constant; C. R. Acad. Sci., Paris, Vol. 260, 1965, p. 6887.

REFERENCES

19. K. Yoshino, and C. J. McMahon, Jr.; Met. Trans., Vol. 5, 1974, p. 363.

20. C. L. Briant, H. C. Feng, and C. J. McMahon, Jr.; Met. Trans., Vol. 9A, 1978, p. 625.

21. I. M. Bernstein; Mat. Sci. Eng., Vol. 6, 1970, p. 1.

22. H. Mabuchi, and C. J. McMahon, Jr.; Proc. Int. Symp. on Hydrogen in Metals, Minakami, Japan, 1979, Trans. JIM, Vol. 21, p. 441, 1980.

23. C. J. McMahon, Jr.; Grain Boundaries in Engineering Materials, Proc. 4th Bolton Landing Conference, June, 1974, p. 525, ed. J. L. Walter, J. H. Westbrook, D. A. Woodford.

24. K. L. Moloznik, C. L. Briant, and C. J. McMahon, Jr.; Corrosion-NACE, Vol. 35, No. 7, 1979, p. 331.

25. C. J. McMahon, Jr. and L. Marchut; J. Vac. Sci. Tech.; Vol. 15, No. 2, 1978, p. 450.

26. J. Kameda, and C. J. McMahon, Jr.; Met. Trans., Vol. 11A, 1980, p. 91.

27. C. L. Briant, and S. K. Banerji; Met. Trans., Vol. 10A, 1979, p. 1729.

28. B. J. Schulz, and C. J. McMahon, Jr.; in "Temper Embrittlement of Alloy Steels", ASTM STP 499, ASTM, 1972, p. 104-135.

29. C. L. Briant, and S. K. Banerji; Met. Trans., Vol. 10A, 1979, p. 123.

30. J. Yu, and C. J. McMahon, Jr.; Met. Trans., Vol. 11A, 1980, p. 277.

31. J. Yu; Ph.D. Thesis, University of Pennsylvania, 1979.

32. R. Viswanathan, and S. J. Hudak, Jr.; Met. Trans., Vol. 8A, 1977, p. 1633.

33. D. P. Dautovich, and S. Floreen; Met. Trans., Vol. 4, 1973, p. 2627.

34. T. D. Lee, T. Goldenberg, and J. P. Hirth; Met. Trans., Vol. 10A, 1979, p. 199.

35. T. D. Lee, T. Goldenberg, and J. P. Hirth; Met. Trans., Vol. 10A, 1979, p. 439.

36. M. Nagumo, H. Morikawa, and K. Miyamoto; Proc. Int. Symp. on Hydrogen in Metals, Minakami, Japan, 1979; Trans. JIM, Vol. 21, 1980, p. 405.

REFERENCES

37. S. Hinotani, F. Terasaki, and F. Nakasato; same as Ref. 36., p. 421.

38. Y. Takeda, and C. J. McMahon, Jr.; University of Pennsylavnia, Philadelphia, 1980. (Submitted to Met. Trans. A).

39. K. Farrell, and A. G. Quarrell; J. Iron Steel Inst., Dec., 1964, p. 1002.

40. G. Sandoz; Met. Trans., Vol. 3, 1972, p. 1169.

41. G. Sandoz; In Hydrogen in Metals, Proc. Int. Conf., Paris, 1972, p. 335.

42. W. W. Gerberich, and Y. T. Chen; Met. Trans., Vol. 6A, 1975, p. 271.

43. H. G. Nelson, and D. P. Williams; in Stress Corrosion Cracking and Hydrogen Embrittlement of Iron Base Alloys, Proc. Conf., Firminy, France, 1973, NACE 1977.

44. W. G. Clark, Jr.; Westinghouse Research Laboratories, Scientific paper 75-1E7-MSLRA-P1.

45. W. W. Gerberich, J. Garry, and J. F. Lesser; in Effect of Hydrogen on Behavior of Materials, Proc. Int. Conf., Moran, Wyo, U.S., 1975; AIME, 1976.

46. C. Kemball; Act. Cong. Intern. Catalyse, Paris, Vol. 2, 1961, p. 1811.

47. W. Palczewska, and I. Ratajczykowa; 3rd Int. Cong. Met. Corros., Moscow, Vol. 2, 1966, p. 64.

48. R. P. Gangloff, and R. P. Wei; Scripta Met., Vol. 8, 1974, p. 661.

49. R. P. Gangloff, and R. P. Wei; Met. Trans., Vol. 8A, 1977, p. 1043.

50. D. P. Williams, and H. G. Nelson; Met. Trans., Vol. 1, 1970, p. 63.

51. S. J. Hudak, Jr. and R. P. Wei; Met. Trans., Vol. 7A, 1976, p. 235.

52. H. G. Nelson, D. P. Williams, and A. S. Tetelman; Met. Trans., Vol. 2, 1971, p. 953.

53. R. A. Oriani; 1969. Proc. Conf. Fundamental Aspects of Stress Corrosion Cracking, Ohio State University, p. 32-49. Houston: NACE.

REFERENCES

54. J. R. Rice and M. A. Johnson; in Inelastic Behavior of Solids, ed. M. F. Kannien, McGraw Hill, New York, N. Y., 1970, p. 641.

55. Jun Kameda, and C. J. McMahon, Jr.; University of Pennsylvania, Philadelphia, PA, 1980.

56. Jun Kameda, N. Bandyopadhyay, and C. J. McMahon, Jr.; Proc. Int. Symp. on "Hydrogen in Metals", Minakami, Japan, 1979; Trans. JIM, Vol. 21, 1980, p. 437.

57. F. Nakasoto, and I. M. Bernstein; Met. Trans., Vol. 9A, 1978, p. 1317.

58. T. Takeyama, and H. Takahashi; Proc. Int. Symp. on "Hydrogen in Metals", Minakami, Japan, 1979; Trans. JIM, Vol. 21, 1980, p. 409.

59. I. M. Bernstein; Met. Trans., Vol. 1, 1970, p. 3143.

60. J. K. Tien; in Effects of Hydrogen and Behavior of Materials, A. W. Thompson and I. M. Bernstein, Eds., TMS-AIME, New York, 1976.

61. H. H. Johnson, J. G. Morlet, and A. R. Troiano; Trans. TMS AIME, 1958, Vol. 212, p. 528.

62. J. P. Hirth; Met. Trans., Vol. 11A, 1980, p 861.

63. J. P. Laurent, G. Lapasset, M. Aucouturier, and P. Lacombe; in "H in Metals", Seven Springs, USA, Ed. by I. M. Bernstein and A. W. Thompson; ASM, 1974, p. 559.

64. I. Taguch; Proc. Int. Sypm. on "Hydrogen in Metals", Minakami, Japan, 1979; Trans. JIM, Vol. 21, 1980, p. 225.

65. M. Weinstein and J. F. Elliott; Trans. Met. Soc. AIME, Vol. 227, 1963, p. 382.

66. J. Kameda; University of Pennsylvania, Philadelphia, PA, (to be published).

67. M. L. Jokl, V. Vitek, and C. J. McMahon, Jr.; Acta. Met., Vol. 28, 1980, (in press).

68. J. J. Gilman; Trans. TMS-AIME, Vol. 212, 1958, p. 783.

69. A. Kimura, H. Matsui, and H. Kimura; Proc. Int. Symp. on "Hydrogen in Metals", Minakami, Japan, 1979; Trans. JIM, Vol. 21, 1980, p. 541.

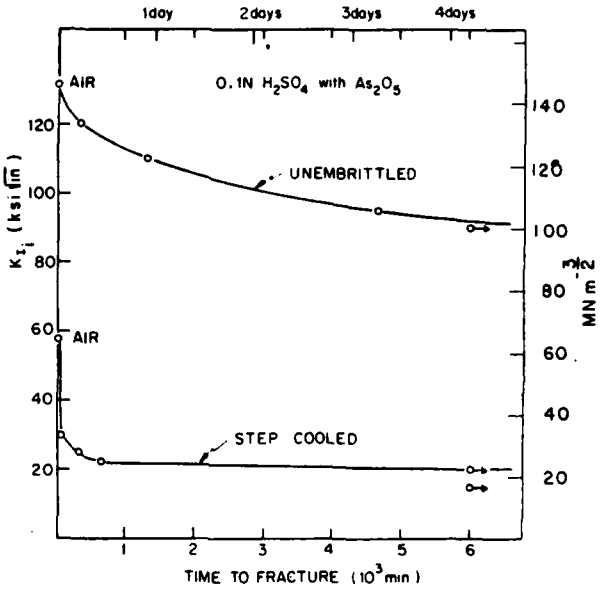

Fig. 1 Time to fracture of pre-cracked cantilever bars of HY 130 steel in a sulfuric acid environment, plotted as a function of initially applied stress intensity. (Ref. 45).

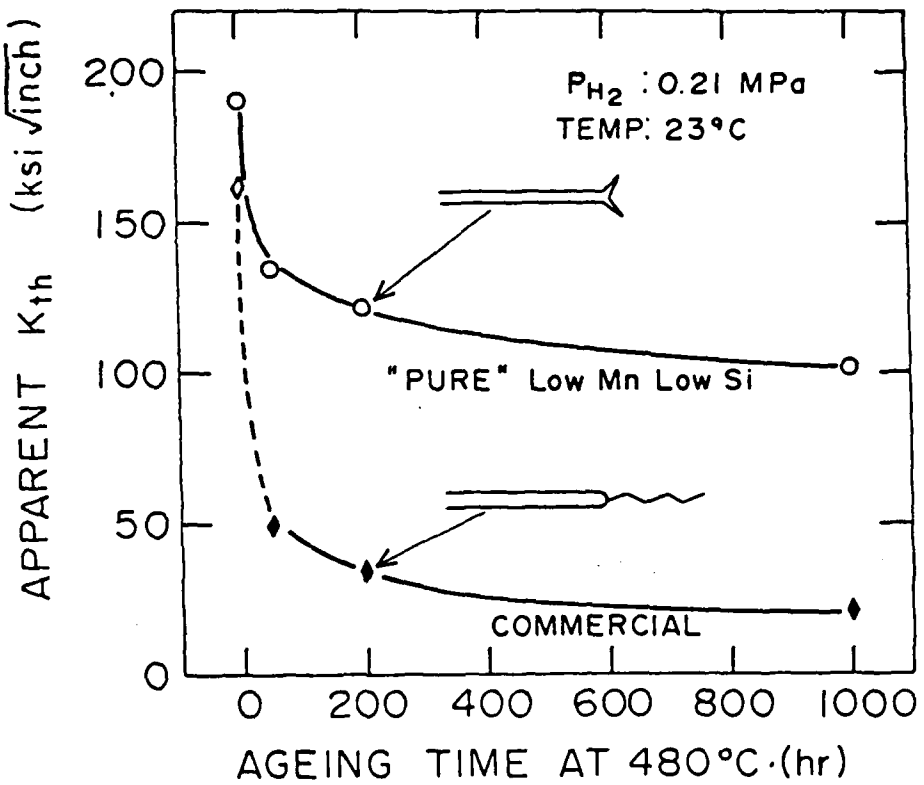

Fig. 2 Threshold stress intensity for detectible crack extension (apparent K_{TH}) in a 0.21 MPa H_2 at 23°C vs. ageing time at 480°C for a pure and a commercial HY 130 steels. (Ref. 56).

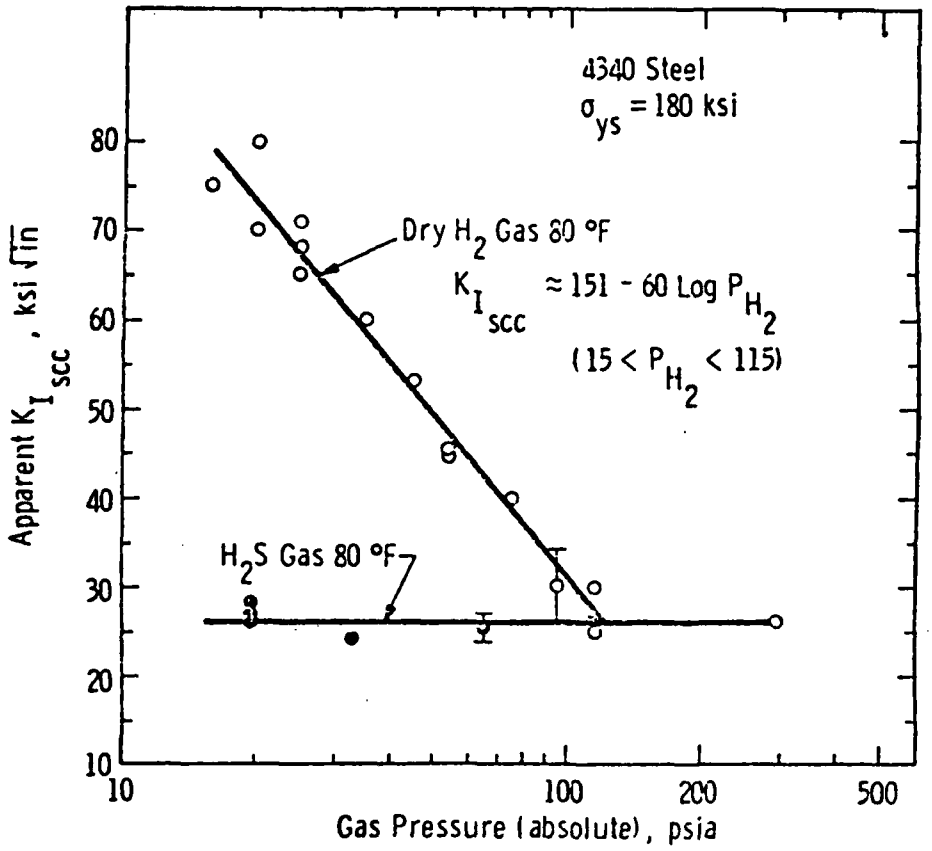

Fig. 3 Variation of apparent K_{ISCC} with H_2 and H_2S gas pressures at 80°F for a 4340-type steel (σ_{YS} = 180 ksi). (Ref. 62).

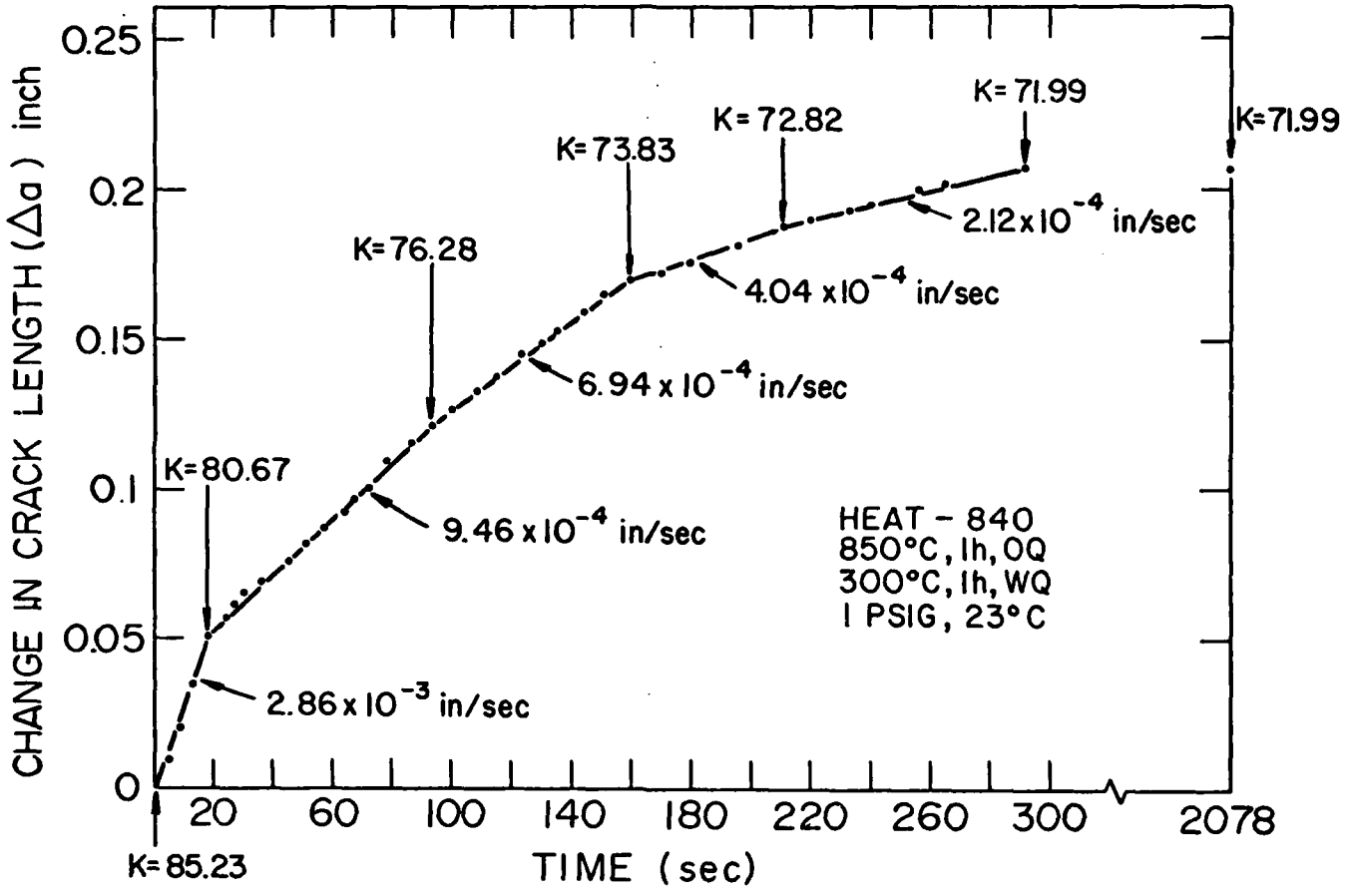

Fig. 4 Example of variation in crack length as a function of time in steel 840 in 0.11 MPa H_2 at 23°C for a a specimen in which a crack arrest was achieved.

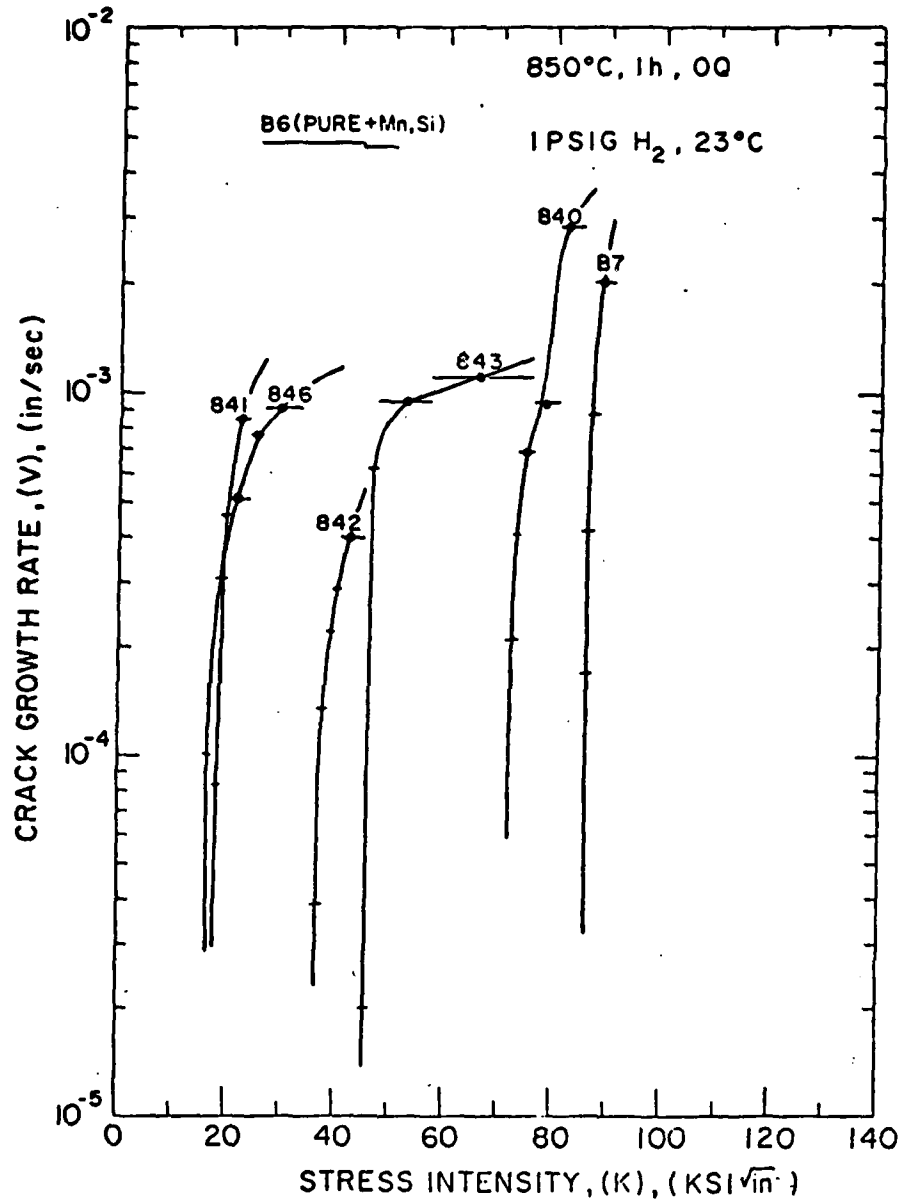

Fig. 5 Variation of crack growth rate as a function of stress intensity in a 0.11 MPa H_2 at 23°C for several steels having yield strength of 1450 MPa.

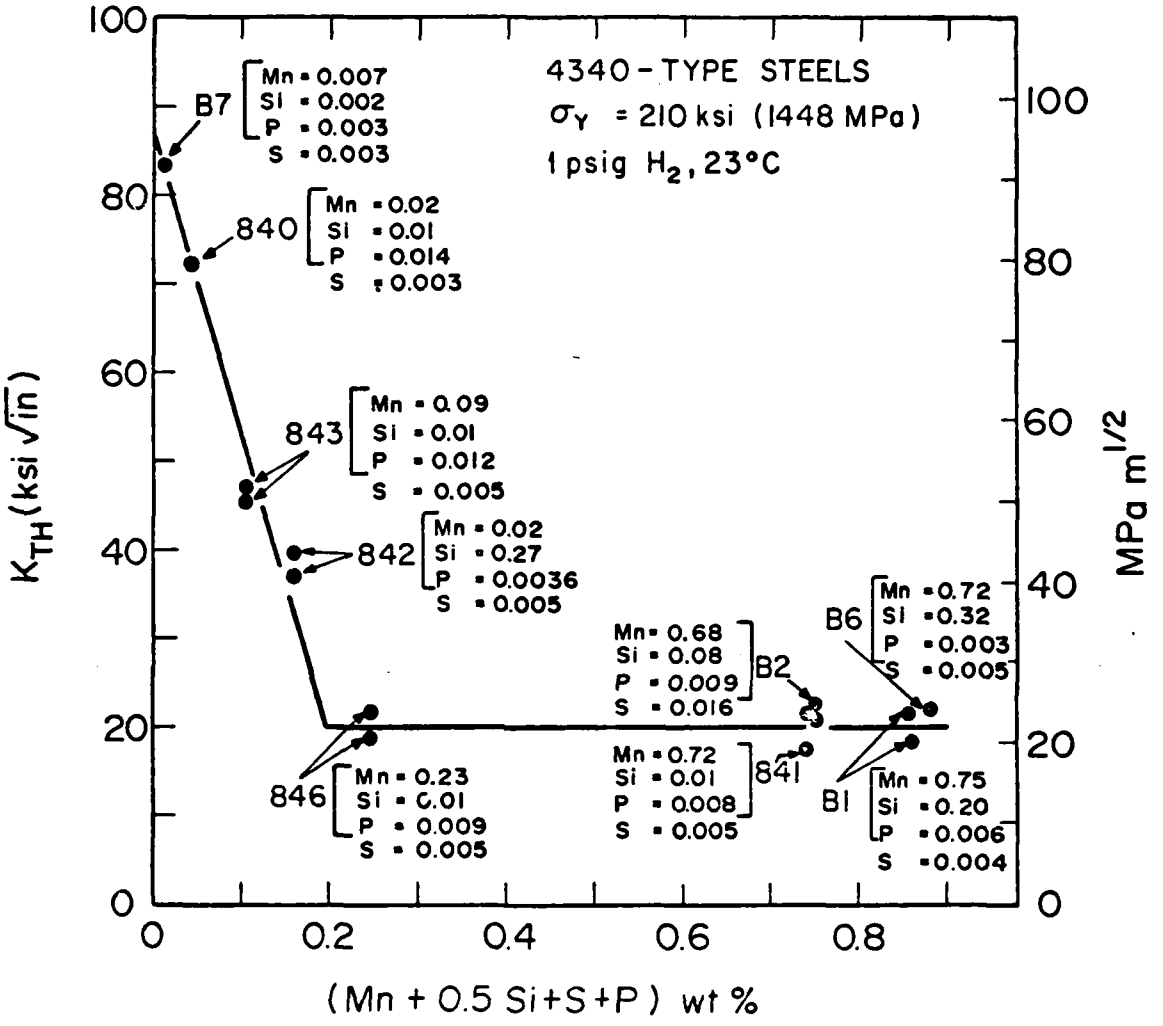

Fig. 6 Dependence of K_{TH} in 0.11 MPa H_2 at 23°C on composition parameter related to segregation tendency of S and P in 4340-type steels of constant yield strength and grain size.

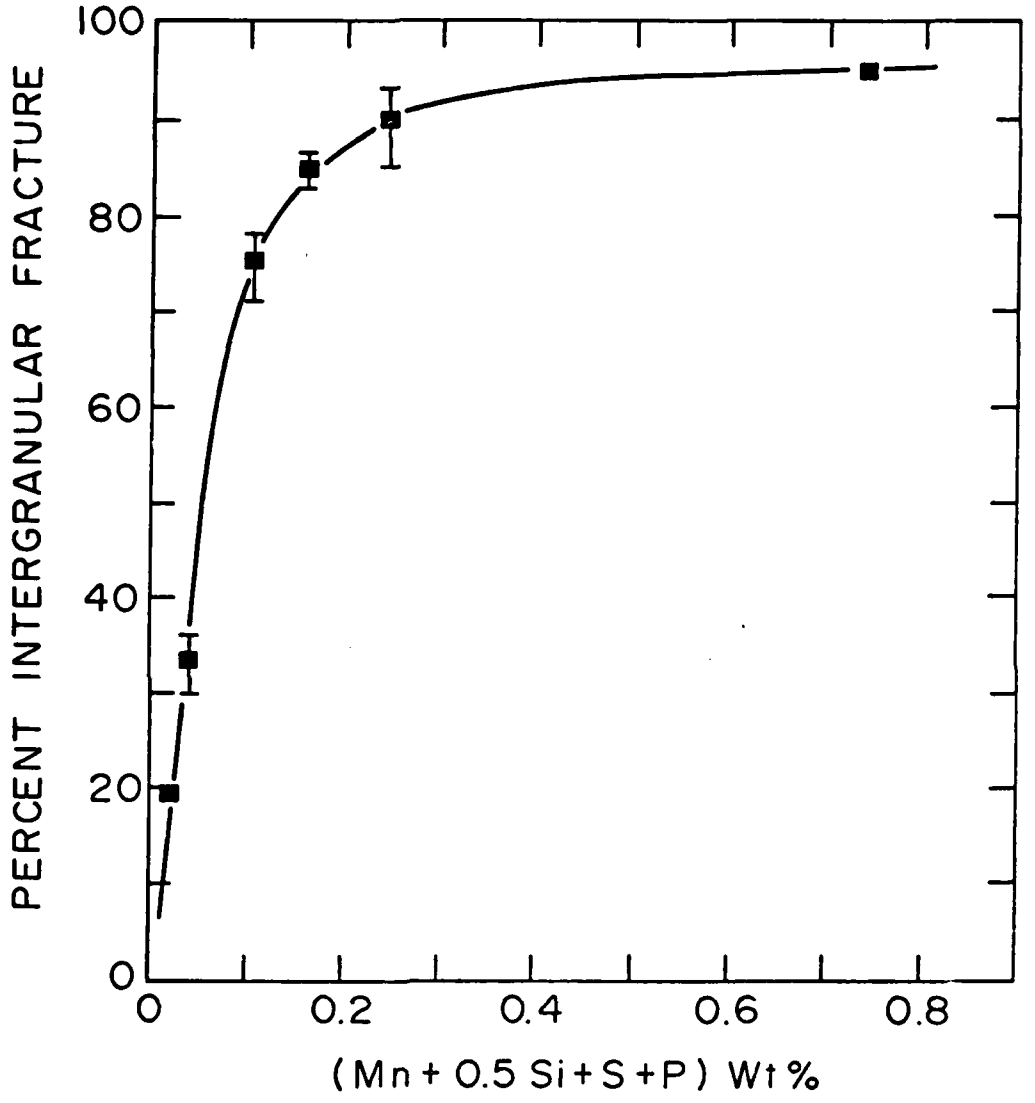

Fig. 7 Corresponding increase in percent intergranular fracture with reduction in K_{TH} value in a 0.11 MPa H_2 at 23°C.

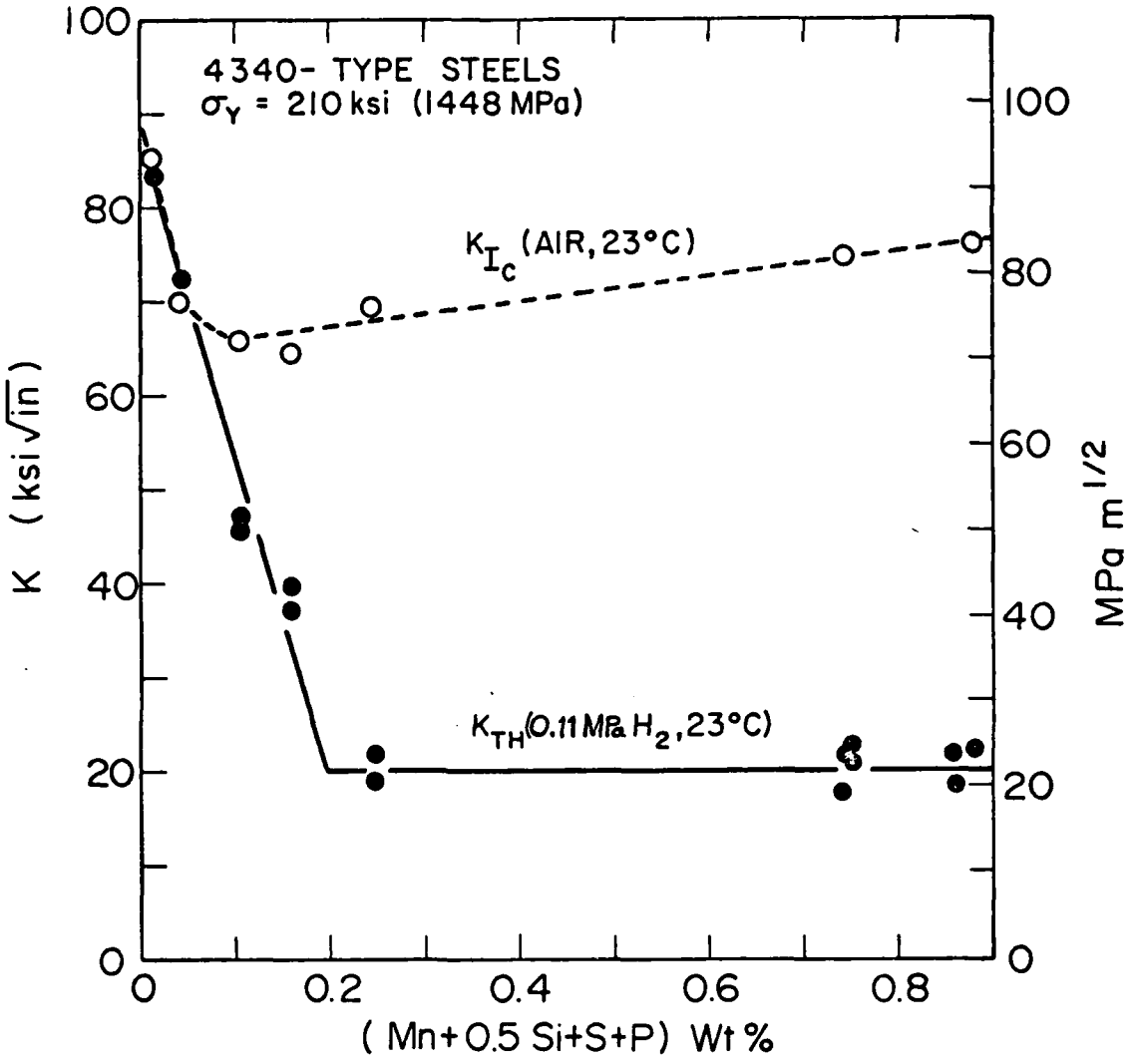

Fig. 8 Dependence of K_{IC} and K_{TH} on composition parameter related to segregating tendencey of S and P in 4340-type steels of constant yeild strength and grain size.

Fig. 9 Scanning electron micrographs of hydrogen-induced fracture surfaces in WOL specimens at three different K_{TH} values in 0.11 MPa H_2 at 23°C
a) ~ 20 ksi$\sqrt{in}$ (22 MPa $\sqrt{m}$)
b) ~ 70 ksi$\sqrt{in}$ (77 MPa $\sqrt{m}$)
c) ~ 85 ksi$\sqrt{in}$ (93 MPa $\sqrt{m}$)

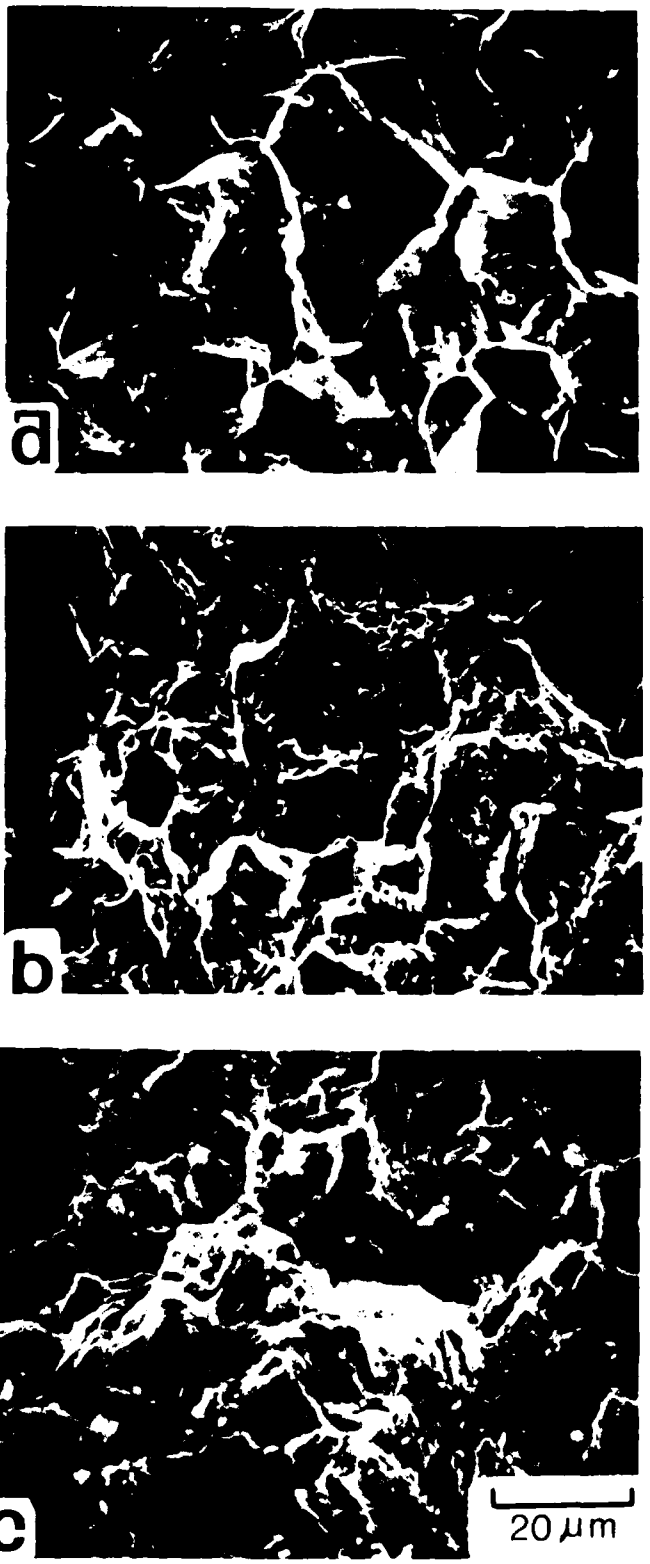
a
b
c
20 μm

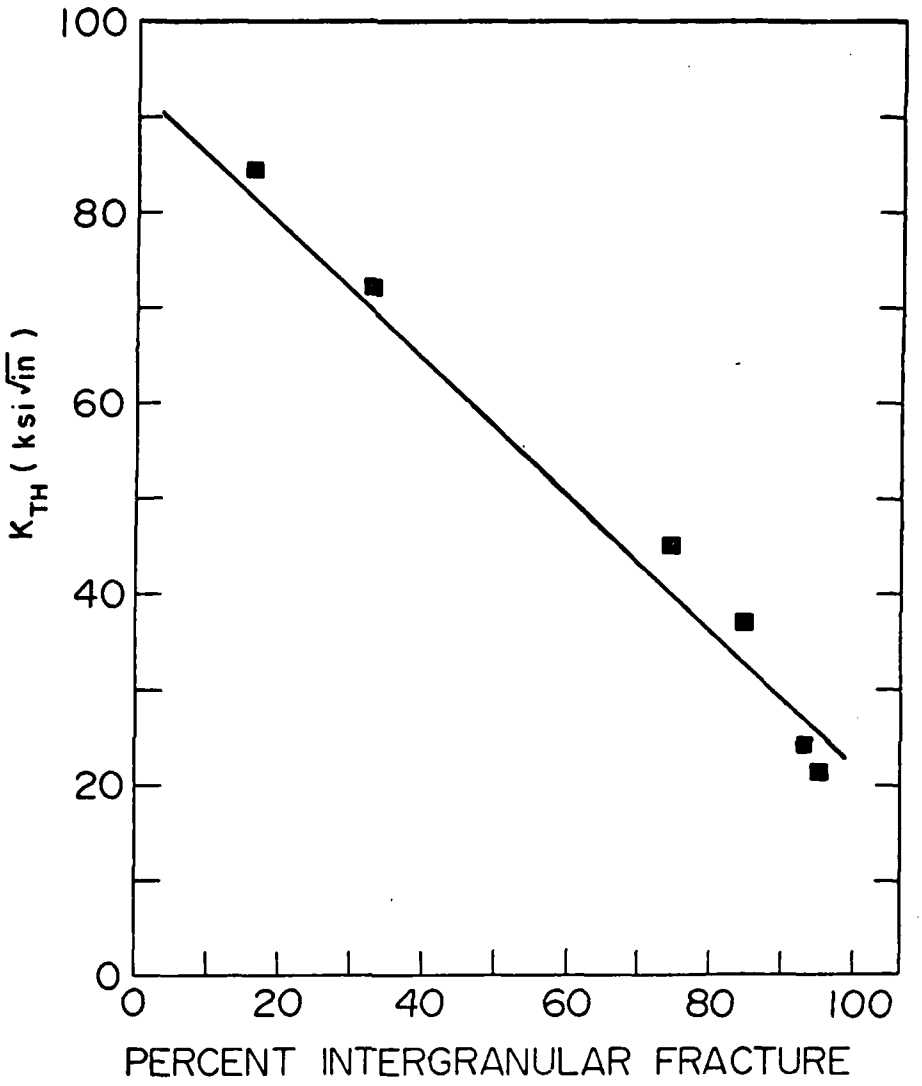

Fig. 10 Relationship between K_{TH} and corresponding percent intergranular fracture in 0.11 MPa H_2 at 23°C for steels with varying amounts of Mn, Si, P and S.

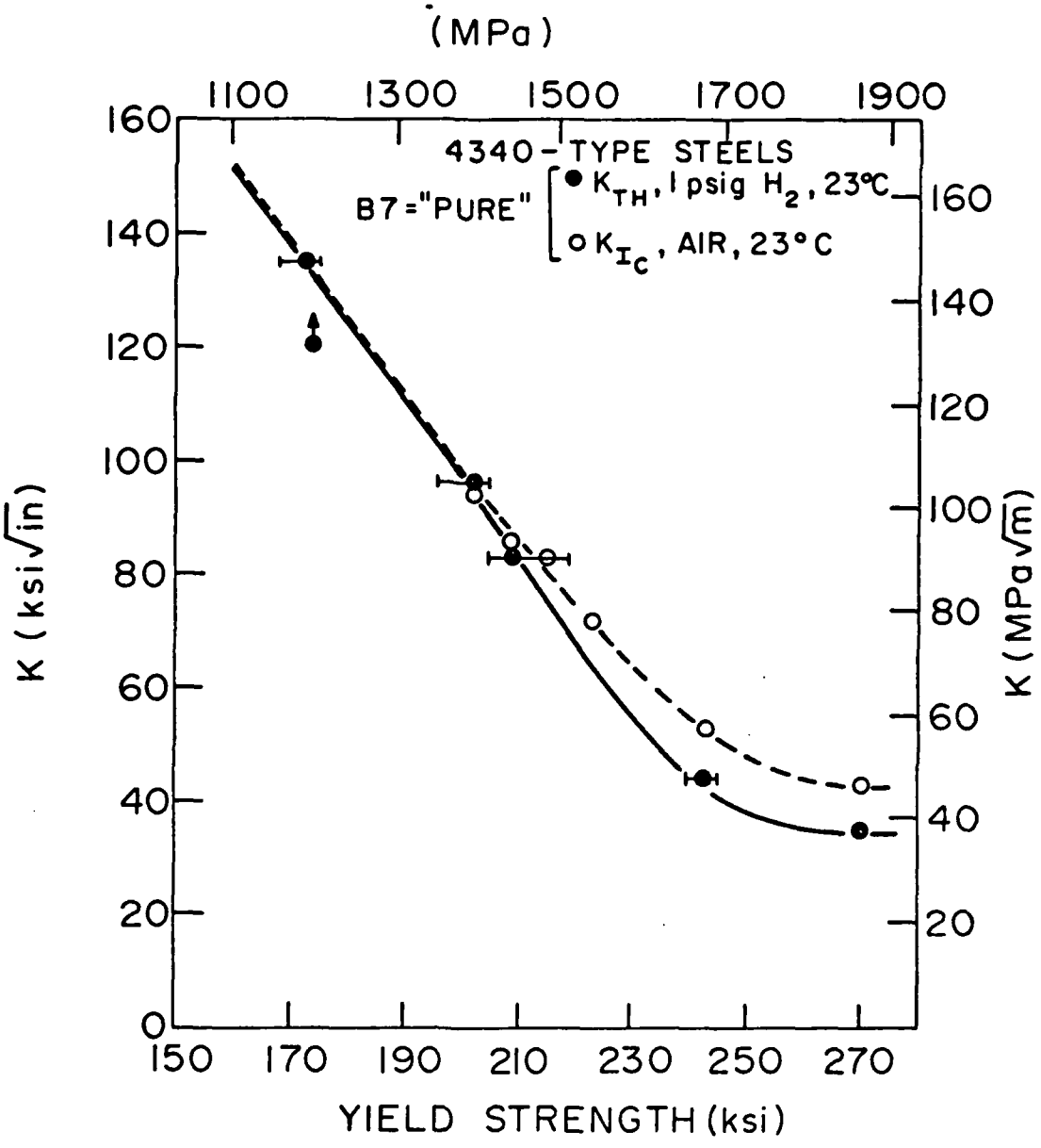

Fig. 11 Variation of K_{IC} in air and K_{TH} in 0.11 MPa H_2 at 23°C with yield strength for pure steel B7.

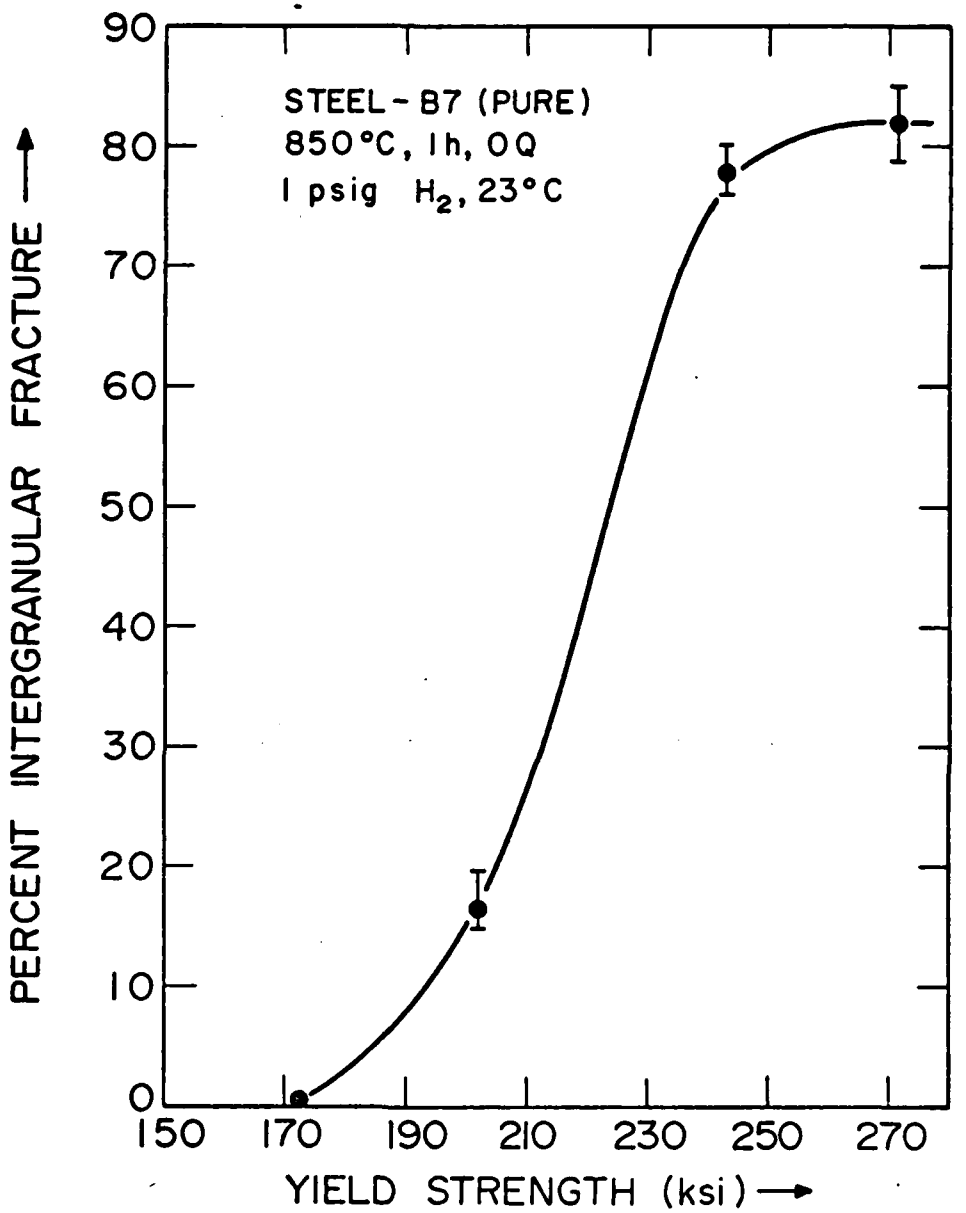

Fig. 12 Variation of percent intergranular fracture in 0.11 MPa H_2 at 23°C with yield strength for pure steel B7.

Fig. 13 Scanning electron micrographs of hydrogen-induced fracture surfaces in WOL specimens of steel B7 at three different strength levels
a) ~ 170 ksi (1170 MPa)
b) ~ 210 ksi (1450 MPa)
c) ~ 270 ksi (1860 MPa)

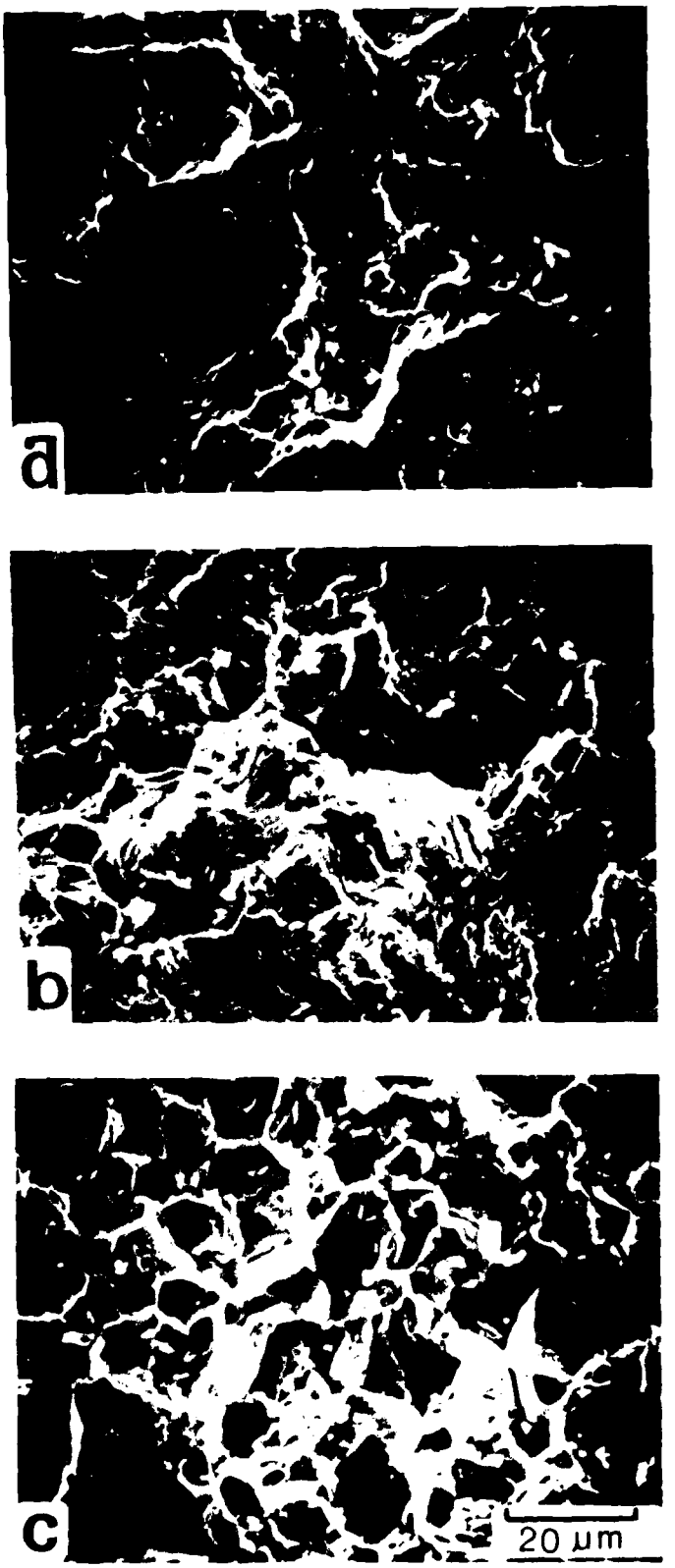
a
b
c
20 µm

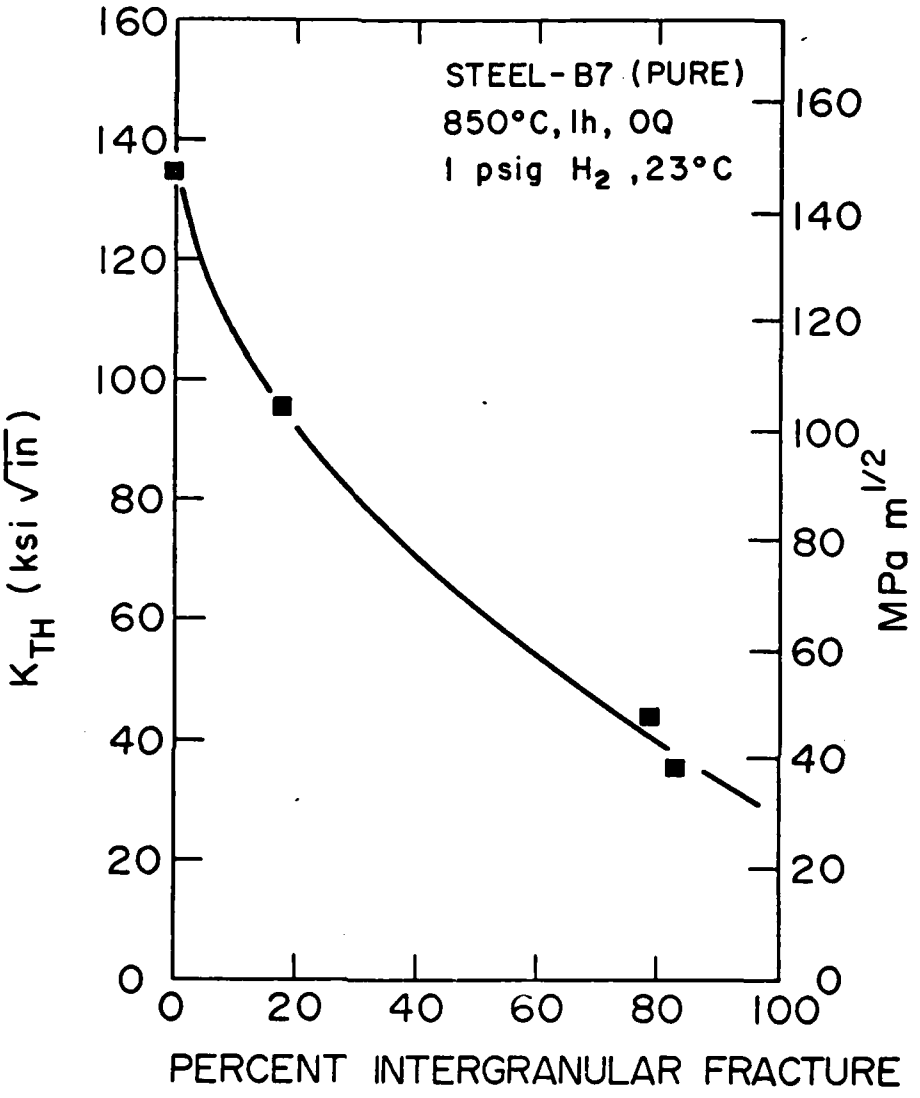

Fig. 14 Relationship between K_{TH} and corresponding percent intergranular fracture in 0.11 MPa H_2 at 23°C for pure steel B7 with varying yield strengths.

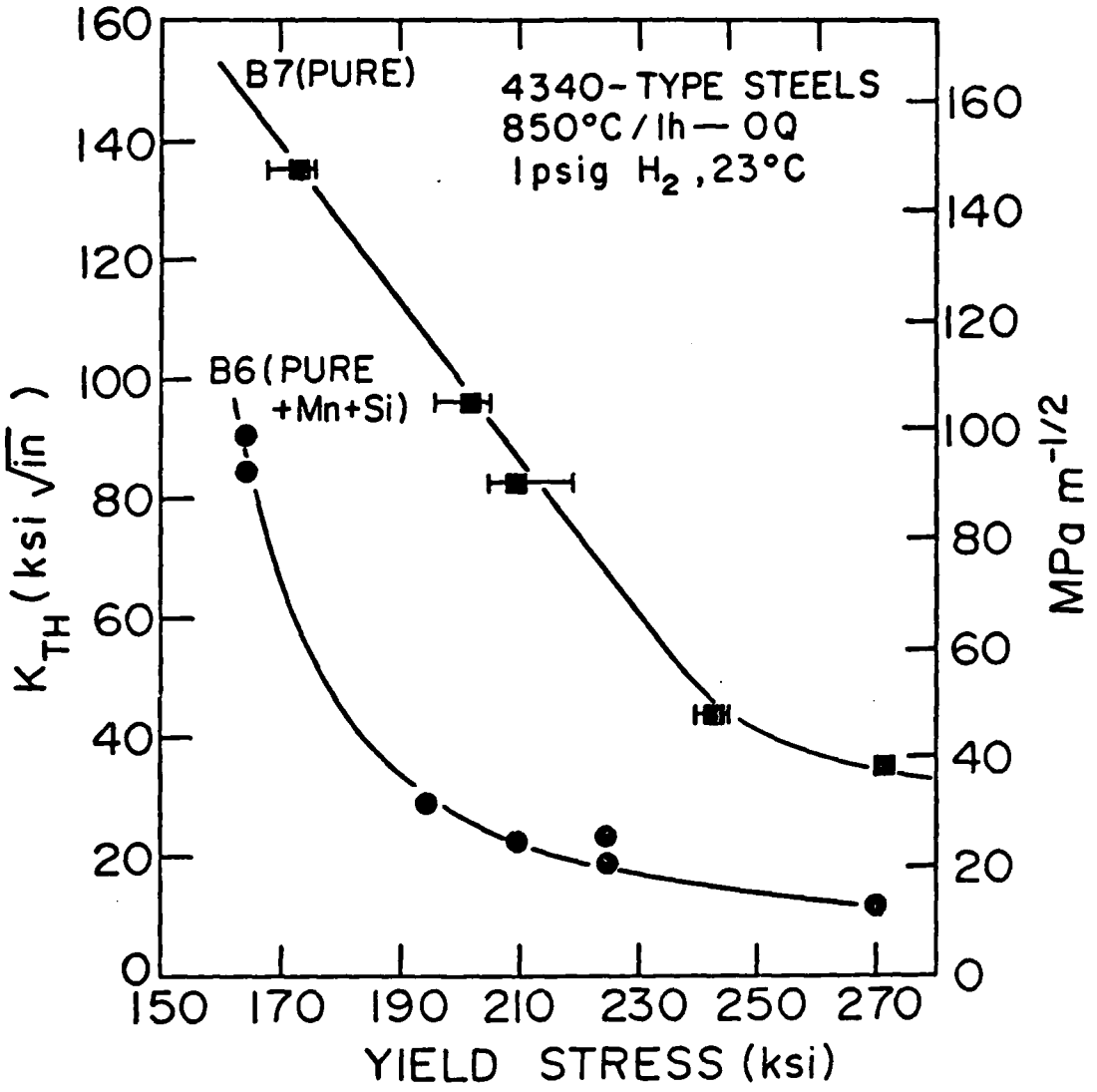

Fig. 15 Variation of K_{TH} in 0.11 MPa H_2 at 23°C with yield strength for Mn- and Si-added pure steel B6 compared with pure steel B7.

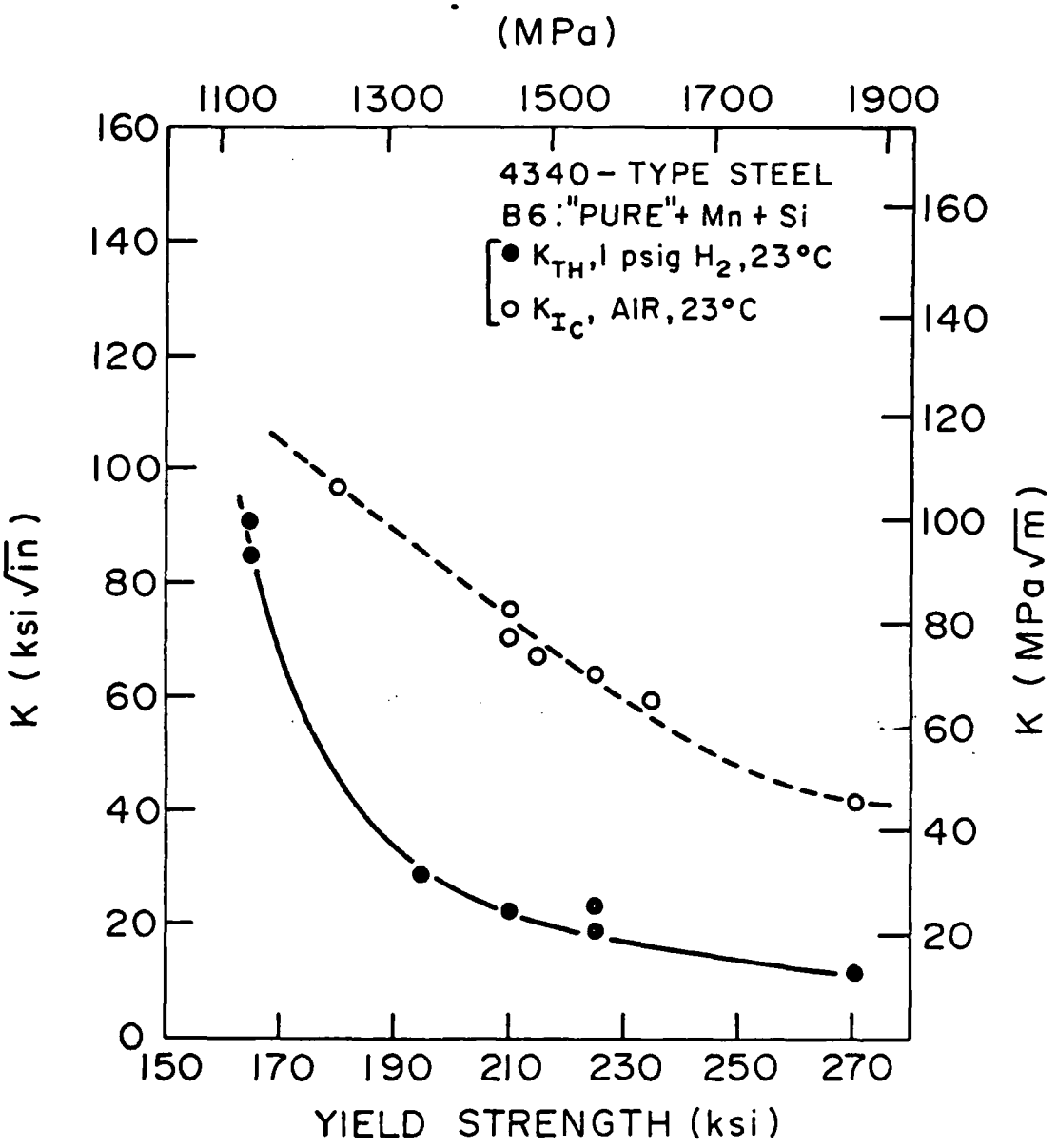

Fig. 16 Variation of K_{IC} in air and K_{TH} in 0.11 MPa H_2 at 23°C with yield strength for steel B6.

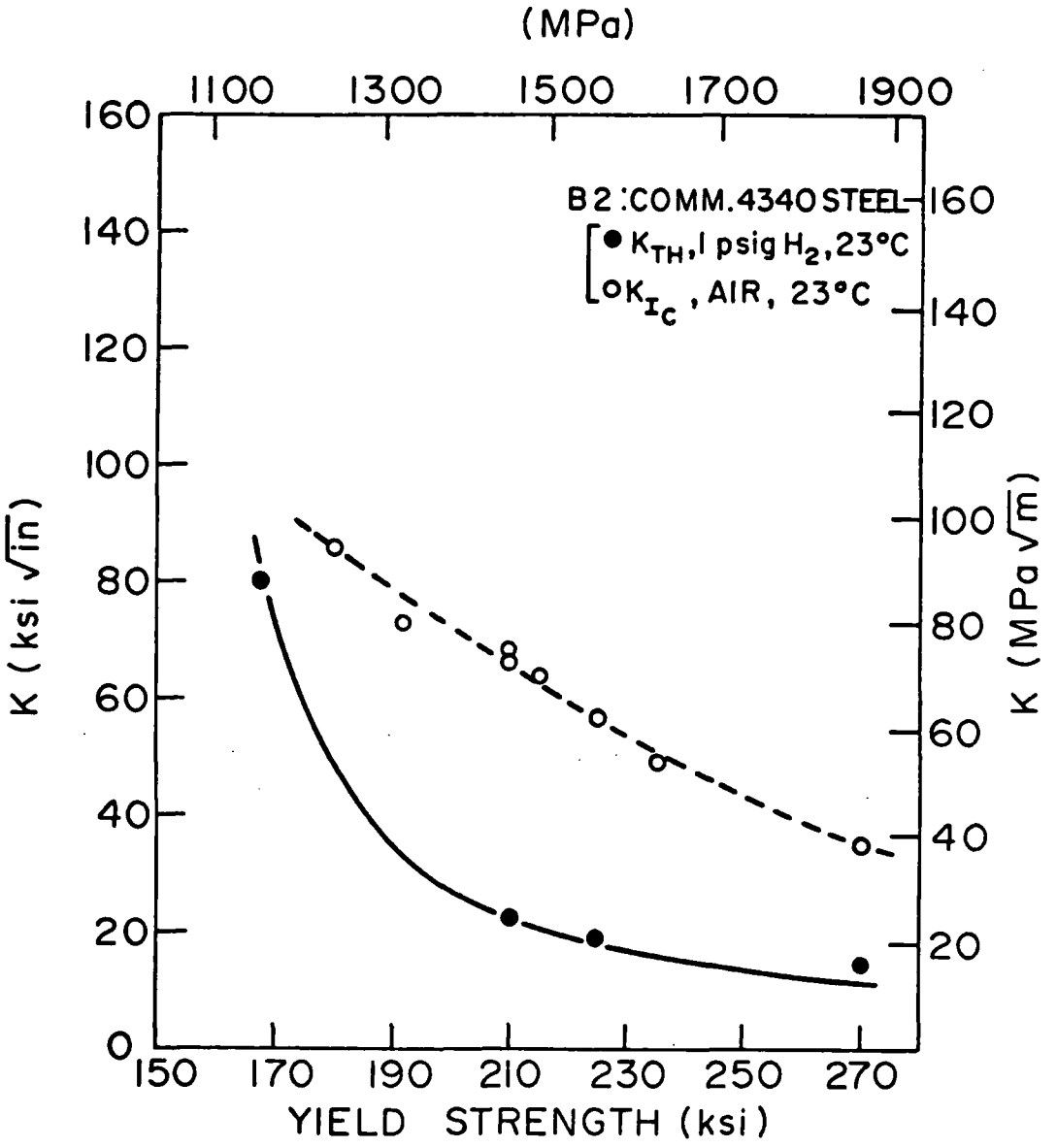

Fig. 17 Variation of K_{IC} in air and K_{TH} in 0.11 MPa H_2 at 23°C with yield strength for commercial steel B2.

Fig. 18 Scanning electron micrograph of hydrogen-induced fracture surface in WOL specimen of steel B6 at low strength level (~170 ksi, 1170 MPa), showing plasticity-related hydrogen-induced fracture.

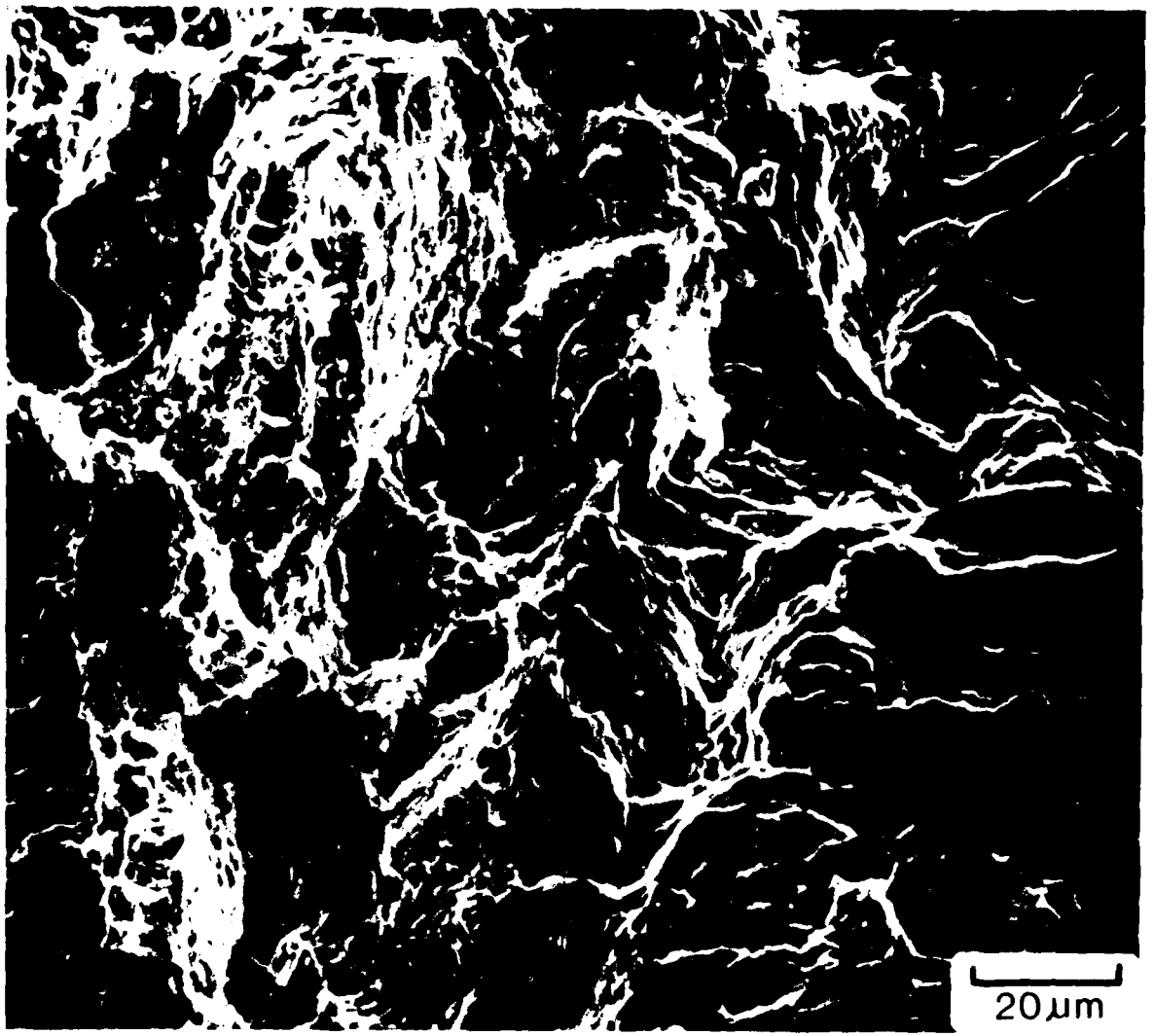
20µm

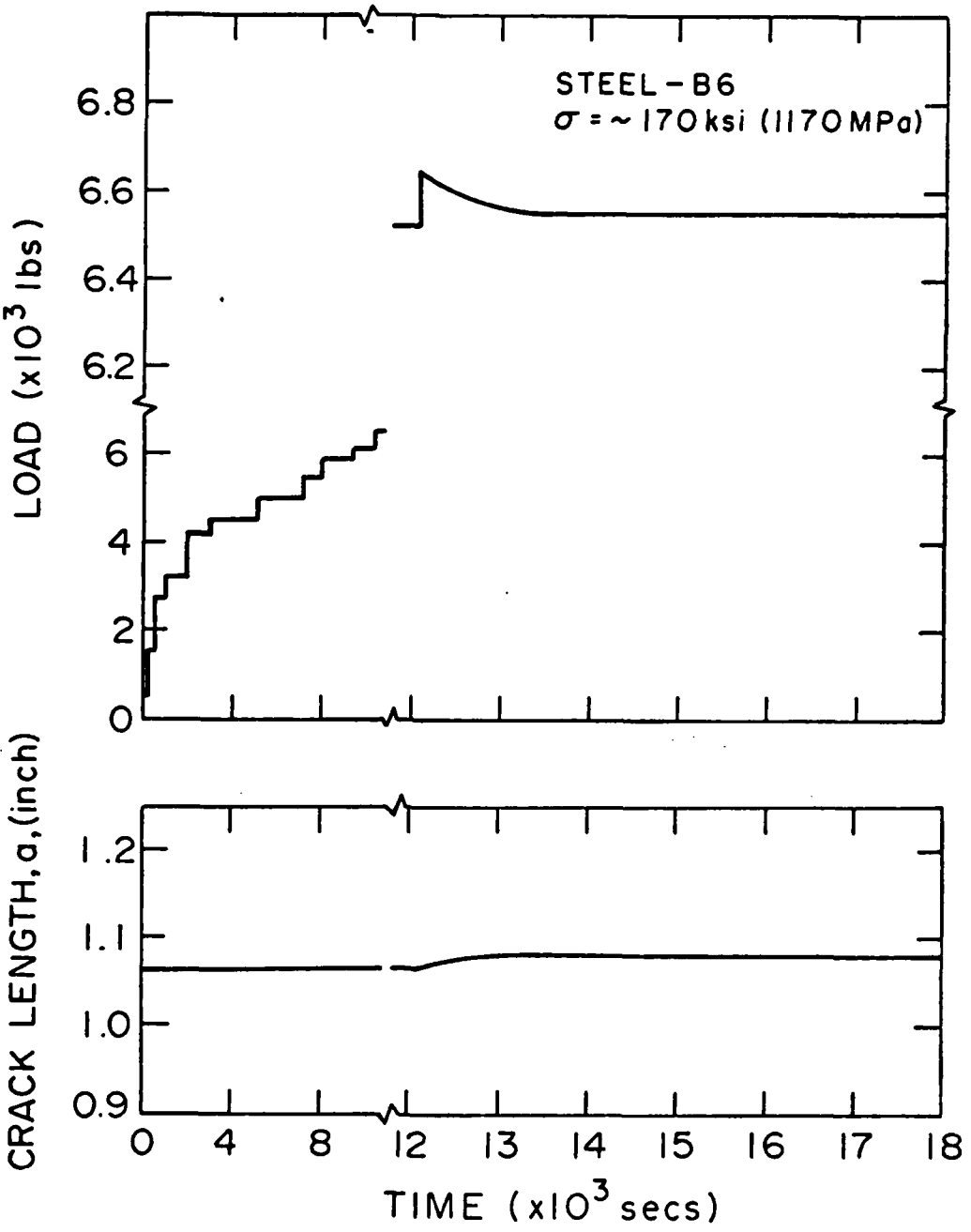

Fig. 19 Variation of bolt load with time showing loding in steps and load-drop at fixed displacement due to crack extension at two yield strength levels for steel B6
a) ~170 ksi (1170 MPa)

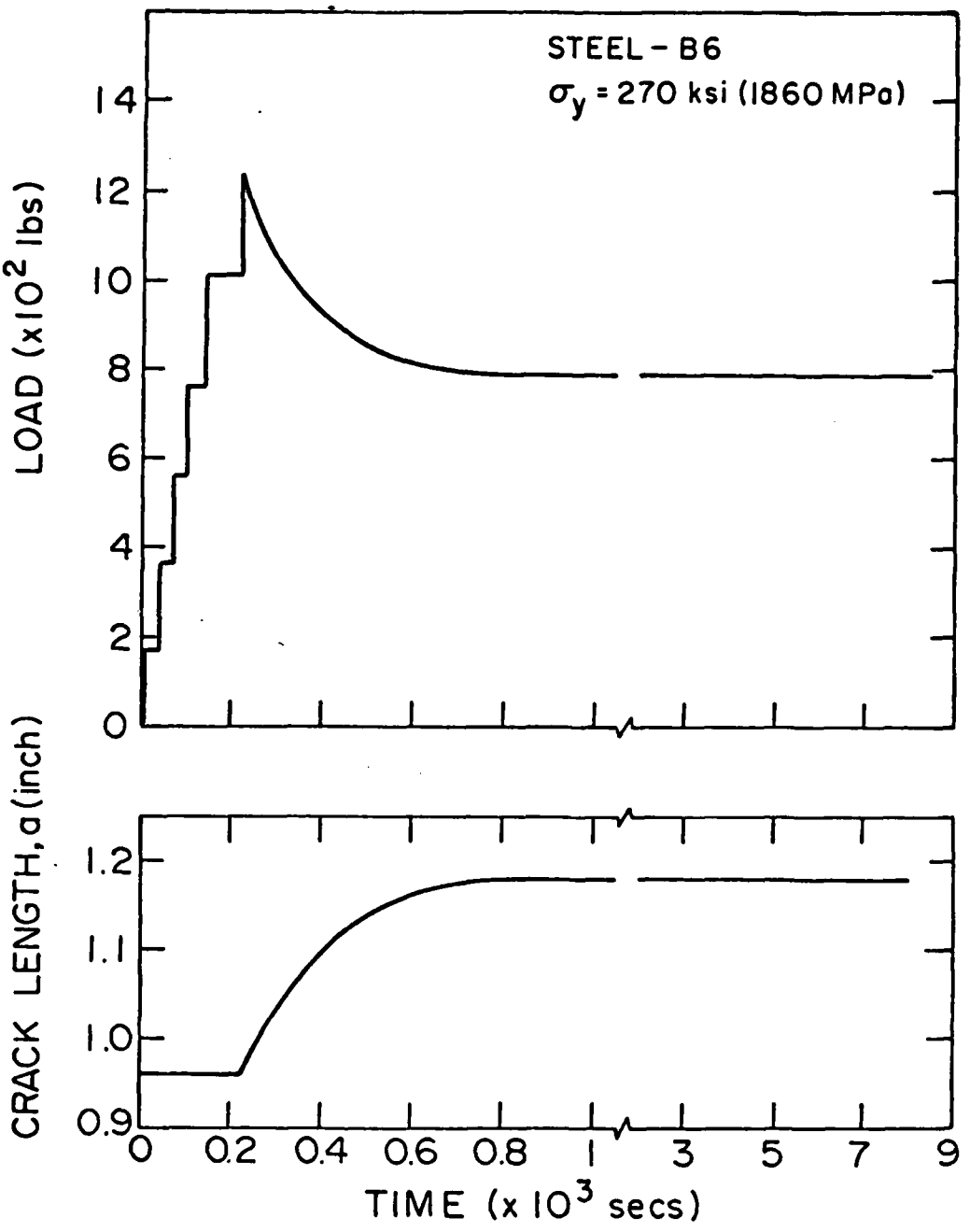

Fig. 19 Variation of bolt load with time showing loding in steps and load-drop at fixed displacement due to crack extension at two yield strength levels for steel B6

b) ~270 ksi (1860 MPa)

Fig. 20 Optical micrographs of hydrogen-induced fracture surfaces at midplane sections showing bifurcation at tip of pre-crack for two types of steels at low strength level (~ 170 ksi, 1170 MPa)
a) Steel B6
b) Steel B7.


a
b
20 µm

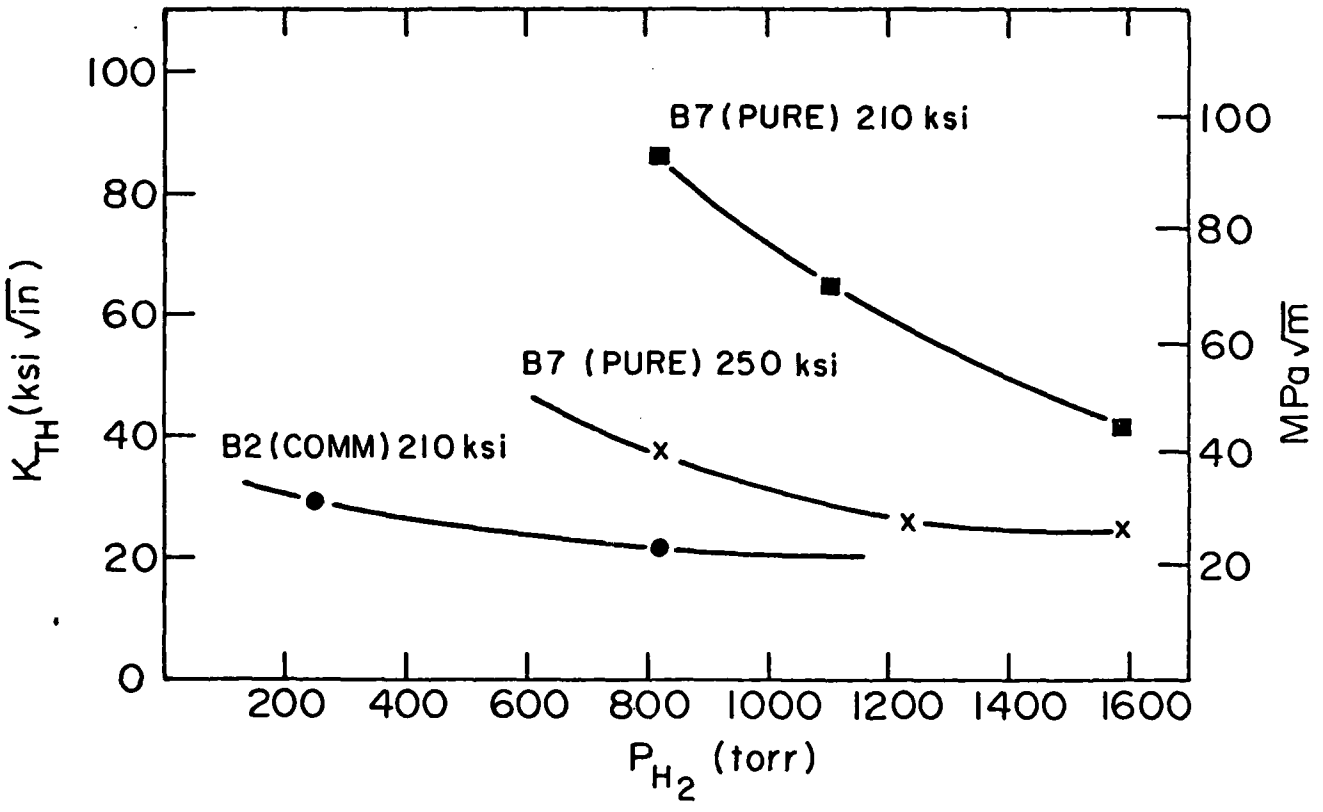

Fig. 21 Variation of K_{TH} with hydrogen pressure at 23°C for commercial steel B2 and pure steel B7 at two different strength levels.

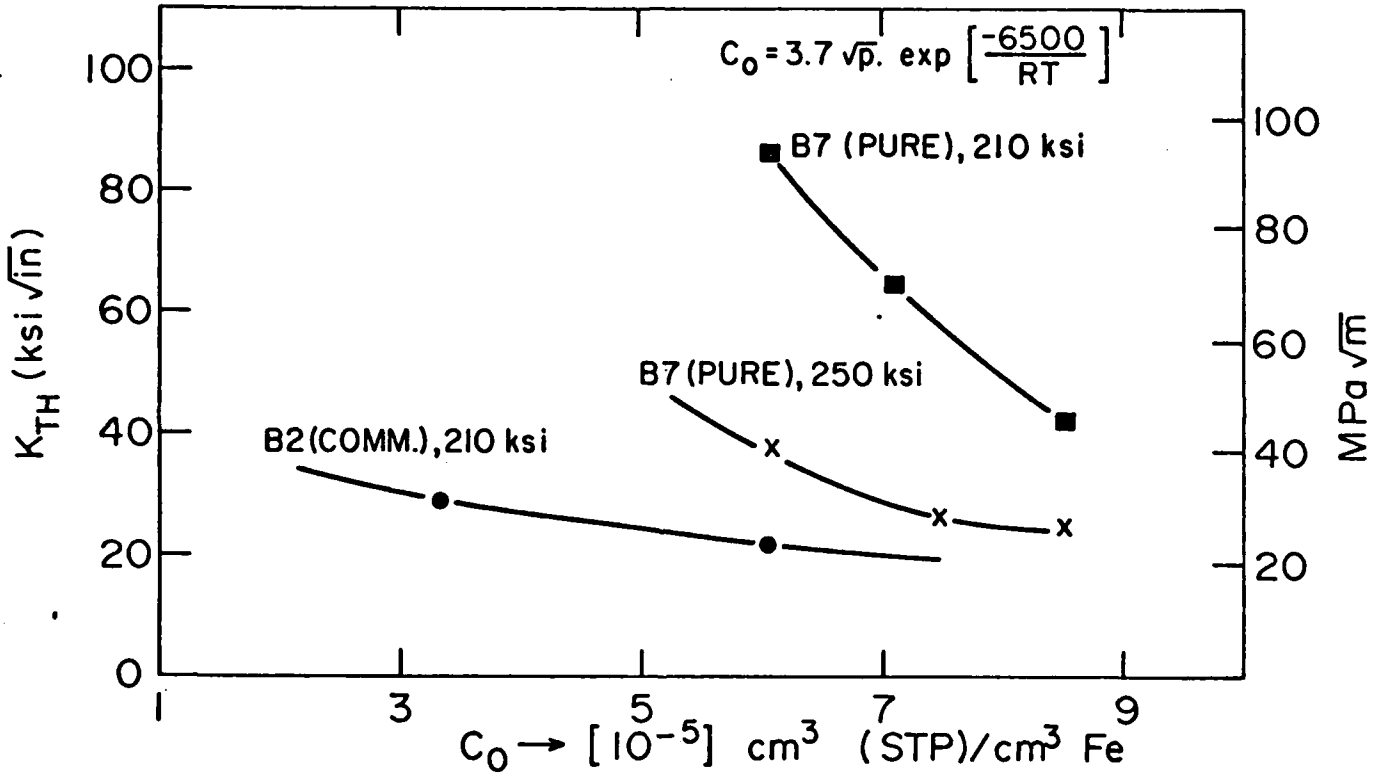

Fig. 22 Variation of K_{TH} with calculated equilibrium solubility of hydrogen (C_o) in unstressed lattice for commercial steel B2 and pure steel B7 at two different strength levels.

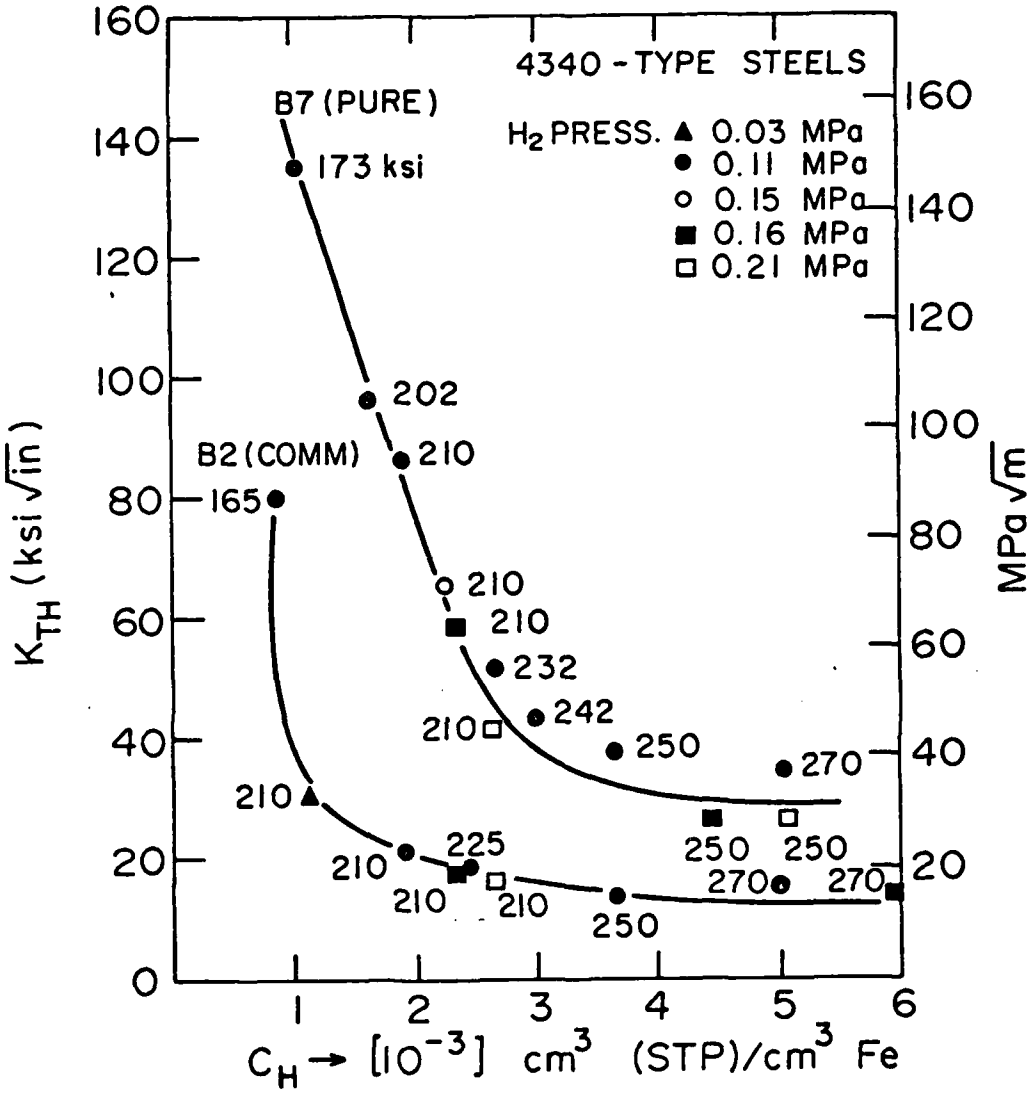

Fig. 23 Dependence of K_{TH} on the calculated maximum H concentration in 4340-type steels for two levels of purity. Data points obtained by varying strength and hydrogen pressure independently.

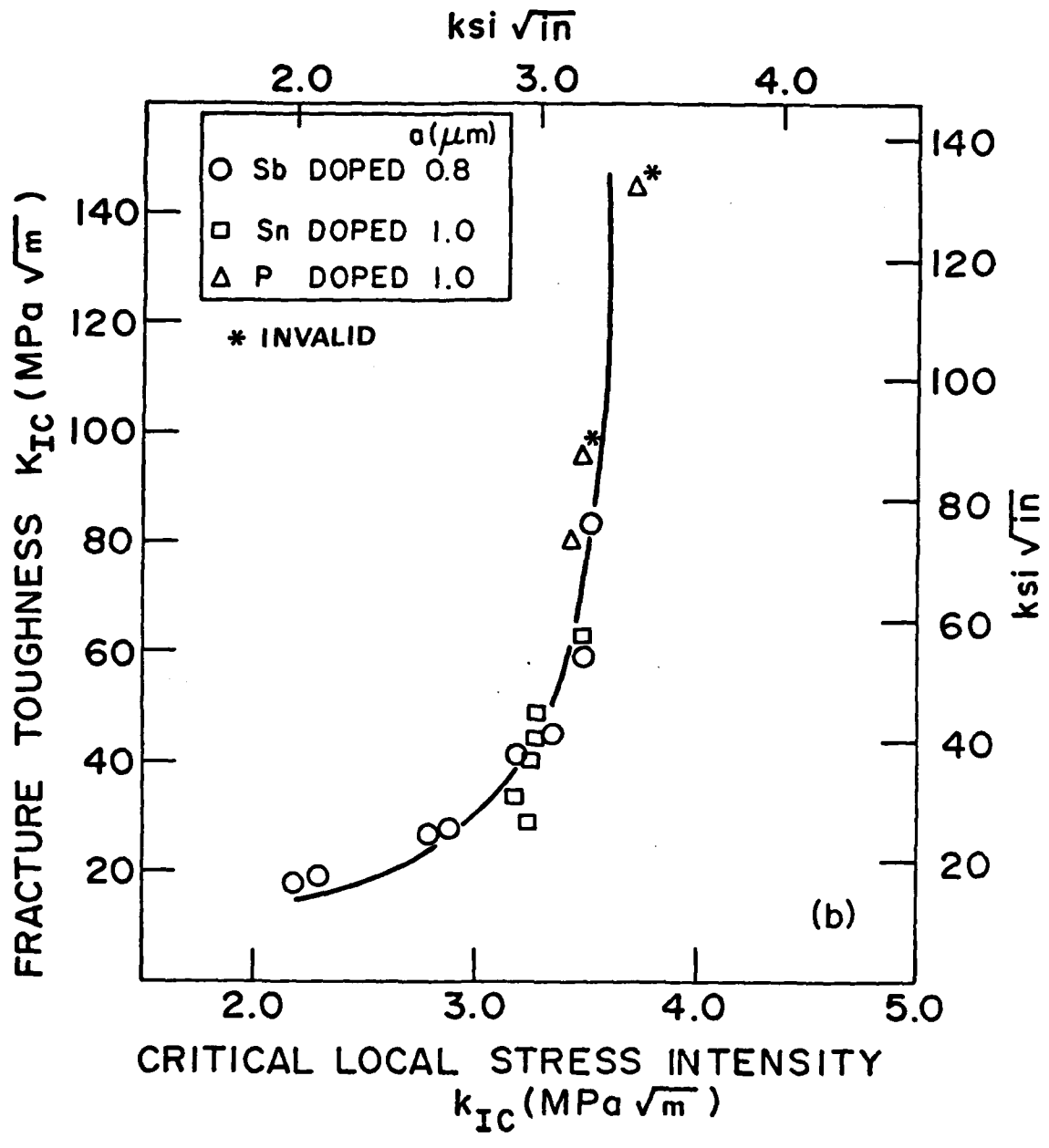

Fig. 24 Dependence of critical local mico-stress intensity k_{IC} on fracture toughness K_{IC} for Sb, Sn and P-doped steels. (Ref. 128).

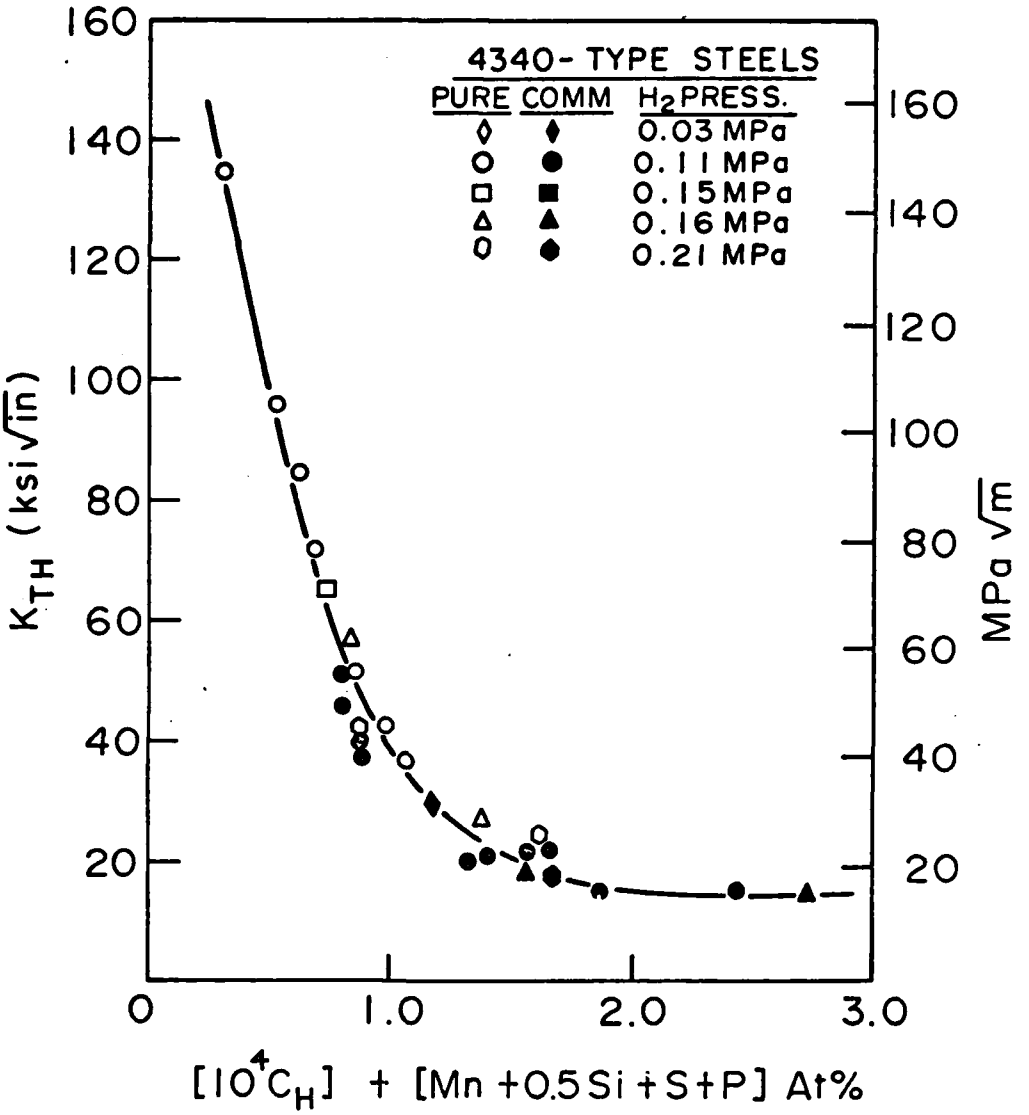

Fig. 25 Dependence of K_{TH} on a parameter which sums both calculated maximum H concentration and a composition parameter related to segregating tendency of S and P in 4340-type steels. Data points obtained by varying composition, strength and hydrogen pressure independently.

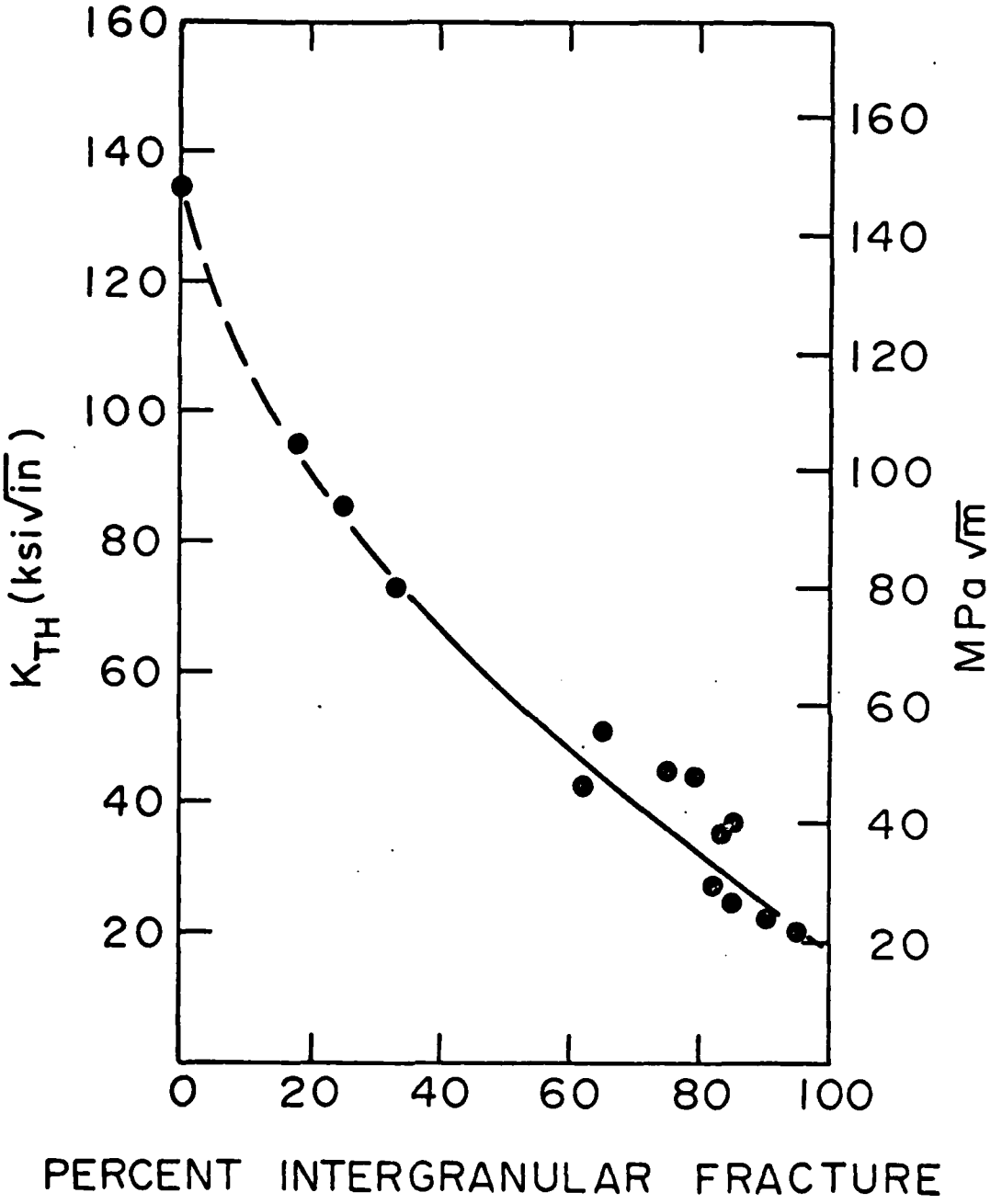

Fig. 26 Relationship between K_{TH} and corresponding percent intergranular fracture in hydrogen. Data points obtained by varying composition, strength and hydrogen pressure independently.